

## **ABSTRACT**

HUANG, JIN SEN. Mechatronics Design of Portable and Lightweight Wearable Robots. (Under the direction of Dr. Hao Su).

Wearable robots have been shown to have rehabilitative abilities due to their ability to produce precise repetitive motion providing needed physical therapy to patients with mobility problems due to stroke, spinal cord injury, or other types of motor function disability. Dunkelberger et al. (2022) However, due to the wide encompassing field of robotics, many research would need to focus on the mechatronics design before proceeding further which is also a large research endeavor that requires a long time and many completed design details are only known to the designers themselves and cannot be used in other research endeavors. Wearable robots can have a greater challenge since a human is a part of the robotic system that places more constraints on the overall design of the robot. Thus in this thesis, I present the mechanical design improvements that was done on the current version of knee exoskeleton developed by the Biomechatronics and Intelligent Robotic Lab (BIROLab) using finite element analysis, 3D modeling, and the lab's current manufacturing resources. The new version of knee exoskeleton was assembled and experimentally evaluated for its reliability and comfort, and its overall mass was reduced from 3.5 kg to 1.25 kg while the overall size decreased approximately 10 cm while allowing for ground clearance when kneeling that was not possible before with the existing exoskeleton. Experimental evaluations were also done on soft cable tethered actuator to verify its ability to accurately track a given reference torque due to its mechanical complexity. Other wearable robots' mechatronics design developed by the BIROLab will also be compiled and presented to showcase the electronics and control systems of wearable robots overall. The results in this thesis provides a comprehensive overview of the mechanical, electrical, and control design of existing and developing wearable robots in the BIROLab.

© Copyright 2023 by Jin Sen Huang

All Rights Reserved

Mechatronics Design of Portable and Lightweight Wearable Robots

by  
Jin Sen Huang

A thesis submitted to the Graduate Faculty of  
North Carolina State University  
in partial fulfillment of the  
requirements for the Degree of  
Master of Science

Mechanical Engineering

Raleigh, North Carolina  
2023

APPROVED BY:

---

Dr. Andrew Lee  
Co-chair of Advisory Committee

---

Dr. Gregory Buckner  
Co-chair of Advisory Committee

---

Dr. Hao Su  
Co-chair of Advisory Committee

## **ACKNOWLEDGEMENTS**

Thanks to my family and friends for their daily support and assistance. I would not be able to return to school without their help. Big thank you to all the BIRO Lab members. This thesis would have never been completed without their guidance and help. Lastly, I like to thank Prof. Su for the opportunity to work in his lab. His mentorship was invaluable since I have zero experience and knowledge in the robotics field.

## TABLE OF CONTENTS

<b>List of Tables . . . . .</b>	<b>v</b>
<b>List of Figures . . . . .</b>	<b>vi</b>
<b>Chapter 1 INTRODUCTION . . . . .</b>	<b>1</b>
1.1 Background . . . . .	1
1.2 Motivations . . . . .	4
1.3 Thesis Contribution . . . . .	5
<b>Chapter 2 Wearable Robot Overview . . . . .</b>	<b>7</b>
2.1 Electronic Architecture . . . . .	8
2.1.1 Electronics Board . . . . .	10
2.1.2 Arduino Based Architecture . . . . .	12
2.1.3 Small Factor Form Computer with Base Architecture (JPU or Raspberry Pi) . . . . .	14
2.1.4 Real-Time Machine with Base Architecture (Simulink Real-Time Machine) . . . . .	16
2.2 Sensors . . . . .	18
2.2.1 Inertial Measurement Unit . . . . .	19
2.2.2 Footswitch . . . . .	20
2.2.3 Torque Sensor . . . . .	21
2.2.4 Built-in Sensor in Actuator: Encoder + Current . . . . .	21
2.3 Control . . . . .	22
2.3.1 Torque Control . . . . .	22
2.3.2 Current Control . . . . .	23
2.3.3 Position Control . . . . .	23
2.3.4 Experimental Results . . . . .	25
2.3.5 Graphical User Interface . . . . .	27
<b>Chapter 3 Rigid Wearable Robot - Knee Exoskeleton . . . . .</b>	<b>30</b>
3.1 Knee Exoskeleton Development . . . . .	31
3.2 Actuation . . . . .	33
3.2.1 Quasi Direct Drive Actuator . . . . .	34
3.2.2 Actuator Selection . . . . .	36
3.3 Mechanical Design Improvements . . . . .	37
3.3.1 Finite Element Analysis . . . . .	37
3.3.2 Wearable Structure . . . . .	41
3.3.3 Final Mechanical Design . . . . .	45
3.4 Experimental Result . . . . .	48

<b>Chapter 4 Soft Wearable Robot - Tethered Actuator Based Exoskeleton . . . . .</b>	<b>52</b>
4.1 Mechanical Design . . . . .	53
4.2 Sensor and Calibration . . . . .	54
4.3 Experiments . . . . .	57
4.4 Application . . . . .	61
<b>Chapter 5 Other Applications . . . . .</b>	<b>63</b>
5.1 Hip Exoskeleton . . . . .	64
5.2 Shoulder Exoskeleton . . . . .	66
5.3 Trans-femoral Prosthesis . . . . .	67
<b>Chapter 6 Conclusion and Future Work . . . . .</b>	<b>70</b>
<b>References . . . . .</b>	<b>72</b>
<b>APPENDICES . . . . .</b>	<b>75</b>
Appendix A      Acronyms . . . . .	76
Appendix B      Units . . . . .	78

## **LIST OF TABLES**

Table 3.1	Comparison of Knee Exoskeleton .....	33
Table 3.2	Comparison of Actuator .....	36
Table 3.3	Knee Exoskeleton Mass Comparison .....	43
Table A.1	A summary of acronyms used in alphabetical order. ....	76
Table B.1	A summary of units used in alphabetical order. ....	78

## LIST OF FIGURES

Figure 2.1	Types of wearable robots developed by the Biomechatronics and Intelligent Robotics Lab . . . . .	8
Figure 2.2	Modular and flexible electronic architecture to control smart actuators using CAN bus communication. . . . .	9
Figure 2.3	Overview of the electronics architecture and the communication method with peripheral sensors and end effectors. PCB (add 7 imu and 8 motors) . . . . .	11
Figure 2.4	Comparison of the size and computational abilities of the three types of architecture that can be used where the micro-controller base architecture can be used alone or with a high level computer. . . . .	12
Figure 2.5	Arduino based micro-controller electronic architecture. . . . .	13
Figure 2.6	Small form factor computer with base electronic architecture. . . . .	15
Figure 2.7	Real time machine with base architecture. . . . .	17
Figure 2.8	All wearable sensor used for wearable robotic system. All sensors can be connected concurrently with our electronics architecture. . . . .	19
Figure 2.9	Three different types of control methods (torque, current, and position) that is commonly used for wearable robots. . . . .	24
Figure 2.10	Torque tracking of a 1 hertz wave at a magnitude of 10Nm as the reference signal where the RMSE is 0.005 Nm. . . . .	25
Figure 2.11	Motor angle tracking of a 1 hertz wave as the reference signal where the RMSE is 0.0025 A. . . . .	26
Figure 2.12	Motor angle tracking of a 1 hertz wave as the reference signal where the RMSE is 0.1312°. . . . .	27
Figure 2.13	Functions of the custom graphical user interface. It is able to set the Bluetooth connection ports as well as to control the estimation model and tuning. The command and sensor data is also plotted in the GUI	29
Figure 3.1	Timeline showing the evolution of our lab's knee exoskeletons. . . . .	31
Figure 3.2	CAD model of the latest knee exoskeleton. . . . .	32
Figure 3.3	Generated mesh for FEA with 24734 tetrahedron elements for calculation. . . . .	38
Figure 3.4	FEA setup for the thigh bar for the knee exoskeleton. . . . .	40
Figure 3.5	FEA of stresses due to 20 Nm actuator on the thigh bar of the knee exoskeleton. . . . .	41
Figure 3.6	Comparison of the current wearable braces with the updated braces.	43
Figure 3.7	Shorten the hook pad for the Velcro straps to increase the range of fit.	44
Figure 3.8	New elastic band design using bungee cord for tension and clip rings to adjust length. . . . .	45
Figure 3.9	CAD model of the new version of knee exoskeleton. . . . .	46
Figure 3.10	CAD model of the new version of knee exoskeleton. . . . .	47

Figure 3.11	Final assembly of the new version of knee exoskeleton that is able to walk and kneel. . . . .	49
Figure 3.12	Torque tracking results with the newly designed knee exoskeleton with an RMSE of 0.0754 Nm. . . . .	50
Figure 3.13	Measured the backdriving torque as the actuator was manually rotated where the max torque required was around 0.17 Nm. . . . .	51
Figure 4.1	Bill of Materials for cable tethered system . . . . .	54
Figure 4.2	Final assembly for the soft tethered actuator. . . . .	55
Figure 4.3	Loadcell calibration using a known torque source. . . . .	56
Figure 4.4	Experimental setup for the soft tethered cable actuator. . . . .	58
Figure 4.5	Torque tracking result for a 10 Nm 1 Hz wave reference signal with a RMSE of 0.008 Nm . . . . .	59
Figure 4.6	Torque tracking result for a 15 Nm 1 Hz wave reference signal with a RMSE of 0.011 Nm . . . . .	60
Figure 4.7	Wrist exoskeleton using a soft tethered actuator that can be used to help open containers for users with arthritis. . . . .	61
Figure 5.1	CAD model of the hip exoskeleton . . . . .	66
Figure 5.2	Back and side views of the shoulder exoskeleton that also uses a soft tethered actuator. . . . .	67
Figure 5.3	Front and side views of the trans-femoral prosthesis. . . . .	69

# CHAPTER

## 1

# INTRODUCTION

## 1.1 Background

Wearable robots like exoskeletons are used to provide active assistance, rehabilitation, or human movement augmentation. For people with mobility problems, such as osteoarthritis and stroke, many lower limb exoskeletons have been developed to provide assistance to help restore their mobility or just to reduce pain, so lower limb exoskeletons can be a non-invasive yet effective treatment. Yu et al. (2019), Lv et al. (2018), Lerner et al. (2017a), Jayaraman et al. (2018) Pediatric versions of lower limb exoskeleton have also been researched to help rehabilitate childhood disabilities, such as Cerebral Palsy (CP), and have

seen treatment success that are comparable to invasive surgery. Chen et al. (2018), Lerner et al. (2017b) Upper limb movement difficulties also poses affect a person's well being. Symptoms, such as paralysis or weakness, due to from injuries or diseases, such as spinal cord injuries or muscular dystrophy, can cause many problems when navigating through daily life as we use our hands and arms the most when interacting with the world. With a vast array of applications, there are also a wide variety type of wearable robots that are specifically designed for certain applications.

For wearable robots such as exoskeletons, they can be separated into two distinct types depending its material which are rigid exoskeletons made of inflexible links and soft exoskeleton, also known as exosuits, made flexible textile materials. Cao et al. (2022) The main benefit of rigid exoskeletons compared to exosuits is that the assistive torque applied by the exoskeleton can be transmitted more effectively. Since current actuators have relatively low output torque without using of heavy gear boxes, the ability to transfer torque from the actuator to the body effectively is a major design consideration because due to the rigidity the exoskeleton can not be fitted to as wide range of body types when compared to the soft, flexible exosuits. The type of exoskeleton can be further discretized by where it is worn on the human body which can further increase the complexity of designing an exoskeleton because each joints and limbs require different assistance profiles.

Other wearable robots like prostheses are separated into different types similar to exoskeletons. However, instead of working with the user in parallel where the user is guiding the exoskeleton, prosthesis needs to replace the missing limb's function, so prosthesis is a device that works in series with the user. Passive prostheses exists and is able to support and work with the wearer in daily life, but for more active activities passive prostheses are not able to keep up with the user. Powered prostheses are able to meet these activity requirements but are far more complex than passive prostheses due to the different fields of study that is required to design a functioning powered prosthesis. Zhu et al. (2022)

Since a robotic system comprises of many different fields of expertise, such as mechanical, electrical, and control systems, each area bring its own design challenges to consider. Designing exoskeletons can be even more difficult because unlike other types of robotic systems, humans are directly in the loop with the robot that requires expertise in control systems and computer science. To also design the exoskeleton to be lightweight and portable, additional design constraints needs to be considered which required expertise in mechanical and electrical engineering.

To provide a solution to the complexities of designing portable, lightweight wearable robots, our exoskeletons are designed to be lightweight and portable to by using a single portable electronic architecture that can power the actuators on all our portable exoskeletons and is able to provide torque up to 20 Nm. The electronic architecture is designed to be modular where it can be used in conjunction with different types high-level controller, remove unnecessary electronic components when not in use, or leave unused sensor ports open. The largest configuration for our electronics has a mass of roughly 1.3 kg making it lighter than most current exoskeleton designs. Plaza et al. (2023) The mechanical design of the exoskeletons also can be adjusted to fit a wide range of body types by using interchangeable lightweight braces instead of increasing mechanical complexities and mass by using a one size fits all method for the wearable structures.

This paper would provide a comprehensive overview of the electronics architecture, the control framework, and its applications through multiple types of wearable robots. As many wearable robots require a specific electronic architecture depending on the type of wearable robot, our flexible electronic architecture design is not limited to the types of wearable robot where it can be used in lower limb exoskeletons, such as knees and hips, as well as upper limb exoskeletons, such as the shoulders. Though the goal is for wearable robotics systems to be portable, the electronic architecture is not limited to portable systems only as currently tethered is still controllable using the same architecture.

## 1.2 Motivations

There are many treatment options for mobility problems, but many options are for more severe cases thus more research is needed to treat milder but still disabling cases. Disabilities can range from gait abnormalities in children with Cerebral Palsy, or adults with age related disorders, such as osteoarthritis and stroke. Many conventional orthoses that are used for these types of population where only a partial assistance is required limits the user's natural movements thus making them uncomfortable. Nesler et al. (2021)

Lower limb exoskeletons (LLE) have been used to provide assistance for people with mobility problems, augmenting healthy individuals' current movement, or even help rehabilitate individuals to regain mobility. LLE are able to support and assist users during locomotion by providing external forces. Lv et al. (2018)

Mechanical design challenges with designing any wearable robot involves in the overall mass and the overall fit of the wearable robot. All wearable robots have inherent mass since it is a physical system thus wearing any additional mass can have an effect on the metabolic cost and natural kinematics of the wearer. For the exoskeleton to be effective, it should be able to overcome this mass penalty and making the wearable robot as lightweight as possible would decrease the mass penalty they incur. Witte and Collins (2020) This creates a major engineering trade off between mass and torque because most lightweight actuators available are not able to produce high torque without using heavy and high inertia mechanisms like gear reducers. The general design of the exoskeleton and its wearable interface, such as the volume and size of the exoskeleton and any wearable braces, also affect the mass of wearable robots.

The fit of wearable robots also has a great effect on the user since the wearable structures are the interface between the robot and the user. Due to the wide range of body type, a one size fits all design is not very feasible for wearable robots. Because unlike regular clothing,

wearable robots are a complex mechanical system where any misfit between the robot and human can have an exponential effect on the control of the system.

Another challenge is the electronic architecture of wearable robots. For exoskeletons to be useful outside of laboratory and clinical setting, a major requirement is for the exoskeleton to be portable. Bae et al. (2018) A challenge for a wearable robotic system to be portable is the power source. The entire system, including all the electronics, sensors, and actuators, must have a stable power source while still be powerful enough to control everything without being tethered or wired to stationary electronics box. A hurdle for powered wearable robotic systems is that simpler, cheaper passive systems, such as braces and orthoses, can perform similar tasks for the wearer as powered systems. This means the control and execution of wearable robots needs to be more robust, adaptable, and accurate when compared to passive systems.

The electronics architecture must be small enough that it would not incur a mass penalty and cause discomfort for the wearer while still be a stable standalone system that is able to be powered by just batteries. Many portable actuator controllers or drivers are commercially available and open source resources are also available. However, commercial options are often built for their own actuators and does not have the flexibility of using other types of actuators, and open source option requires expertise to understand and assemble the architecture from scratch. Duval and Herr (2016)

### **1.3 Thesis Contribution**

The main goal of this thesis is to improve on a current state of the art knee exoskeleton and help develop a soft transmission platform for future wearable application. In parallel with these research goal, the documentation of current wearable robots developed by other member in the BIROLab was also compiled to improve the efficiency of future research in

wearable robotics. Key contributions are as the following.

1. Improved the mechanical design on a current state of art knee exoskeleton by reducing its mass and size while also add in a new kneeling capability.
2. Helped develop an universal soft cable tethered actuation platform that can be used in current and future wearable robotic applications.
3. Introduce a portable and universal electronic architecture that can be used to control modular wearable robots.
4. Performed experimental evaluation of exoskeleton functionality such as torque and force tracking.
5. Compile and summarize the mechatronic design of current wearable robots.

Chapter 2 will provide an overview of the electronics and general design framework of portable wearable robots. Chapter 3 will discuss the development of knee exoskeletons, and the mechanical improvements I made on the current knee exoskeleton for a lighter, more comfortable, and compact knee exoskeleton. Chapter 4 introduce the soft tethered actuator that has been developed to replace rigid tethered transmission and the experimental results using tethered actuation. Chapter 5 will summarize rest of the wearable robots that is currently in development by the lab with chapter 6 concluding the thesis.

## CHAPTER

# 2

## WEARABLE ROBOT OVERVIEW

Since wearable robotics is a multidisciplinary field, research progress requires experts in many fields. For example, a controls engineer may have developed a new gait estimation algorithm, but lack the mechatronic platform to test the algorithm and require the aide from mechanical and electrical engineers to build a suitable wearable robot for testing. Conversely, a mechanical engineer may already built a wearable robot that can be used but require aide in controls which is why collaboration between fields is crucial. However, though many research groups have developed many types of wearable robots, the intricacies of each wearable robot is known only to the designers themselves and integration of any externally developed parts, electronics, or code may not be compatible with each other. The electronic architecture developed by the Biomechatronics and Intelligent Robot lab is

able solve the compatibility problem by being a flexible and modular design that allow for different platforms of high level computing, such as using block-diagram programming in real-time machines, and different types of wearable robots, such as lower limb exoskeletons or prostheses, making it easier to further wearable robotics research which can be seen in Figure 2.1

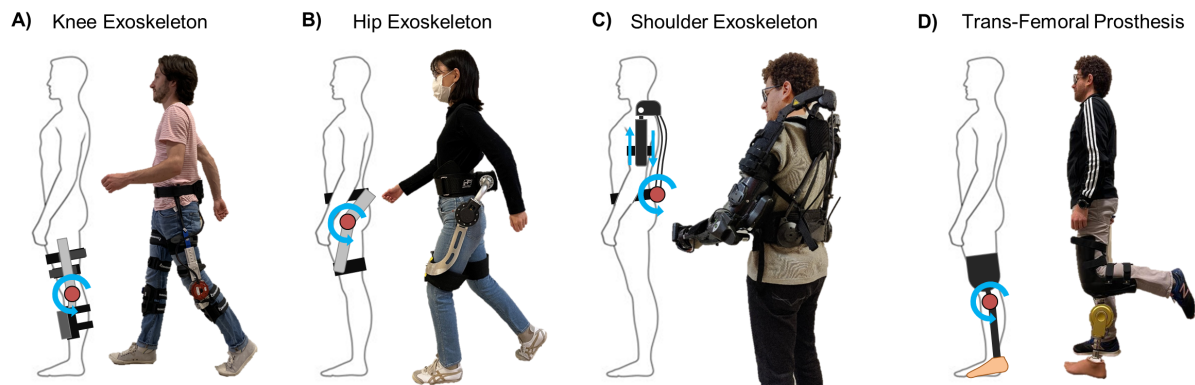


Figure 2.1: Types of wearable robots developed by the Biomechatronics and Intelligent Robotics Lab

## 2.1 Electronic Architecture

An overview of a wearable robot using our singular flexible electronics architecture is described in Figure 2.2. A benefit of the architecture is that not all the components in the system needs to be used if is not needed and no other modification is needed in the hardware or software if a part or sensor is disconnected. The PCB electronics architecture can be thought as a single unifier for the high-level computer before and the wearable robotic applications after where many types of high-level computer and wearable robot can be used together with a single board.

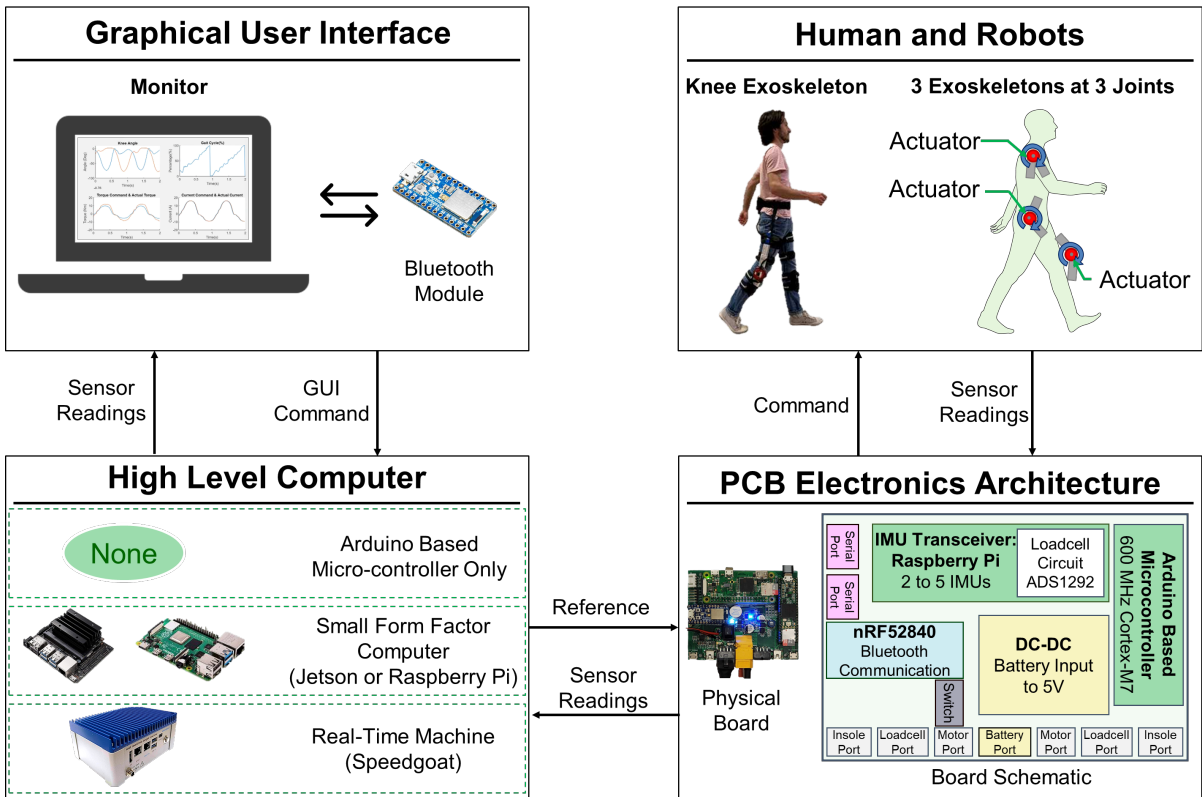


Figure 2.2: Modular and flexible electronic architecture to control smart actuators using CAN bus communication.

### **2.1.1 Electronics Board**

The purpose and duties of a wearable robot's electronics architecture is the ability to read the sensors and drive the actuators quickly to provide proper assistance to the wearer. The architecture should also be able to be powerful enough to run the control algorithms. Duval and Herr (2016) The custom electronics architecture and the communication protocols used to connect the micro-controller to the sensors and actuators can be seen in Figure 2.3.

State of the art controller for wearable robots requires the joint angle and acceleration to compute the torque commands for the actuators. To read these measurements, sensors, such as encoders or inertial measurement units (IMUs), are required; however, using wired sensors will cause chaotic movements in the cables which will be uncomfortable for the wearer. To solve this problem, wireless sensors are used. Our electronics are able to read up to 7 IMUs via Bluetooth. The IMU data and information is received in a Raspberry Pi Zero on the PCB running a custom operating system that specifically written to send the sensor data to the micro-controller through serial communication with a sample frequency of 100 Hz.

Recent developments for wearable robots that uses smart actuators uses CAN bus communication with a predefined communication message that send data from the embedded sensors in the actuator. Typically measurements from the current sensor, torque sensor, and encoder can be sent from the actuators while also able to receive the desired torque or angle position reference. To properly drives these smart actuators, the micro-controller's capabilities with a CAN bus communication module integrated with a customized circuits in the PCB.

It is also crucial to monitor the sensors and wearable robot's information as well as the actuator commands during experiments and tests that involves new control strategies implementation or new users. The electronics architecture also can pass the robot's in-

█ On exoskeleton   
 █ Graphical User Interface   
 █ On PCB   
 █ Adapter

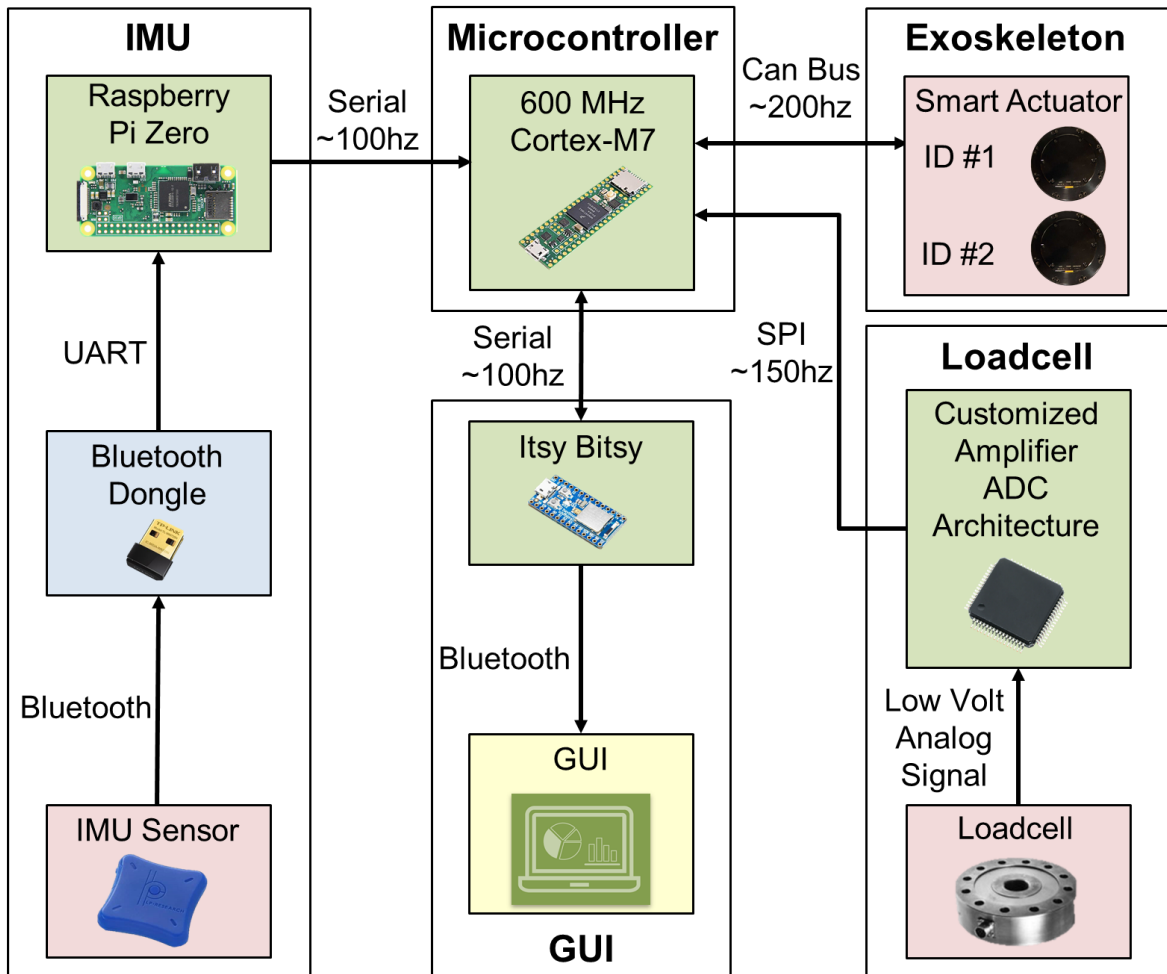


Figure 2.3: Overview of the electronics architecture and the communication method with peripheral sensors and end effectors. PCB (add 7 imu and 8 motors)

formation to a stationary computer via Bluetooth with a sample frequency 100 Hz using Bluetooth antennas embedded in the PCB. The sent information is visualized with an user-friendly GUI.

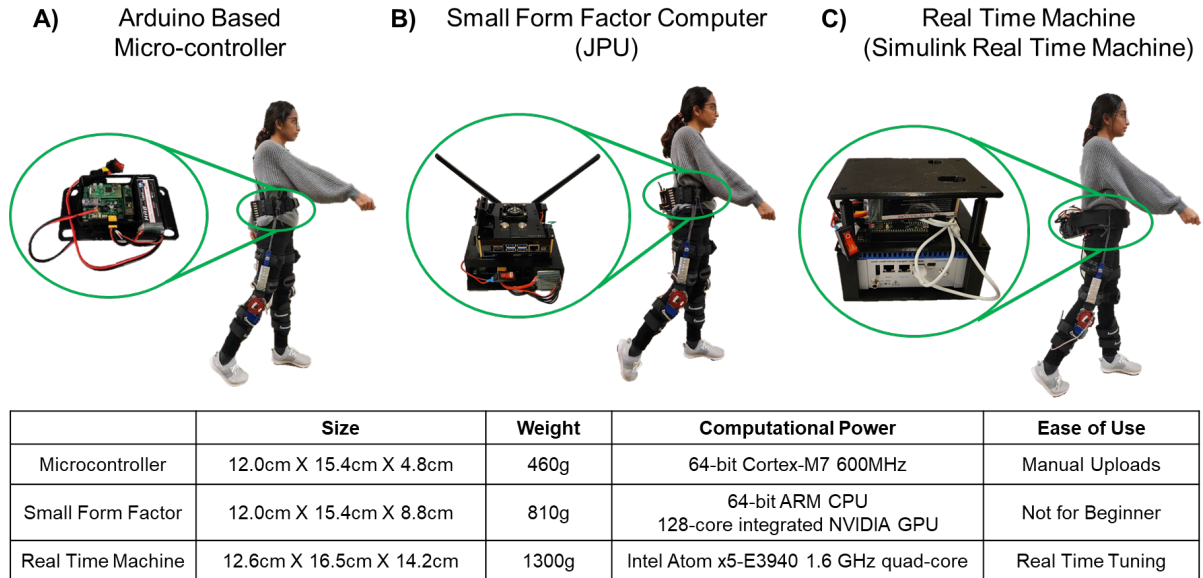


Figure 2.4: Comparison of the size and computational abilities of the three types of architecture that can be used where the micro-controller base architecture can be used alone or with a high level computer.

### 2.1.2 Arduino Based Architecture

The system overview of our electronic architecture can be seen in Figure 2.5. This electronic architecture is flexible and to various needs as it is used in all three types exoskeletons. The custom PCB board allows the individual components to be flexible and modular where it connects to an Arduino based ARM Cortex-M4 micro-controller (Teensy 3.6, 180 MHz), Bluetooth module (Itsy Bitsy), and the Raspberry Pi Zero. This setup can communicate data

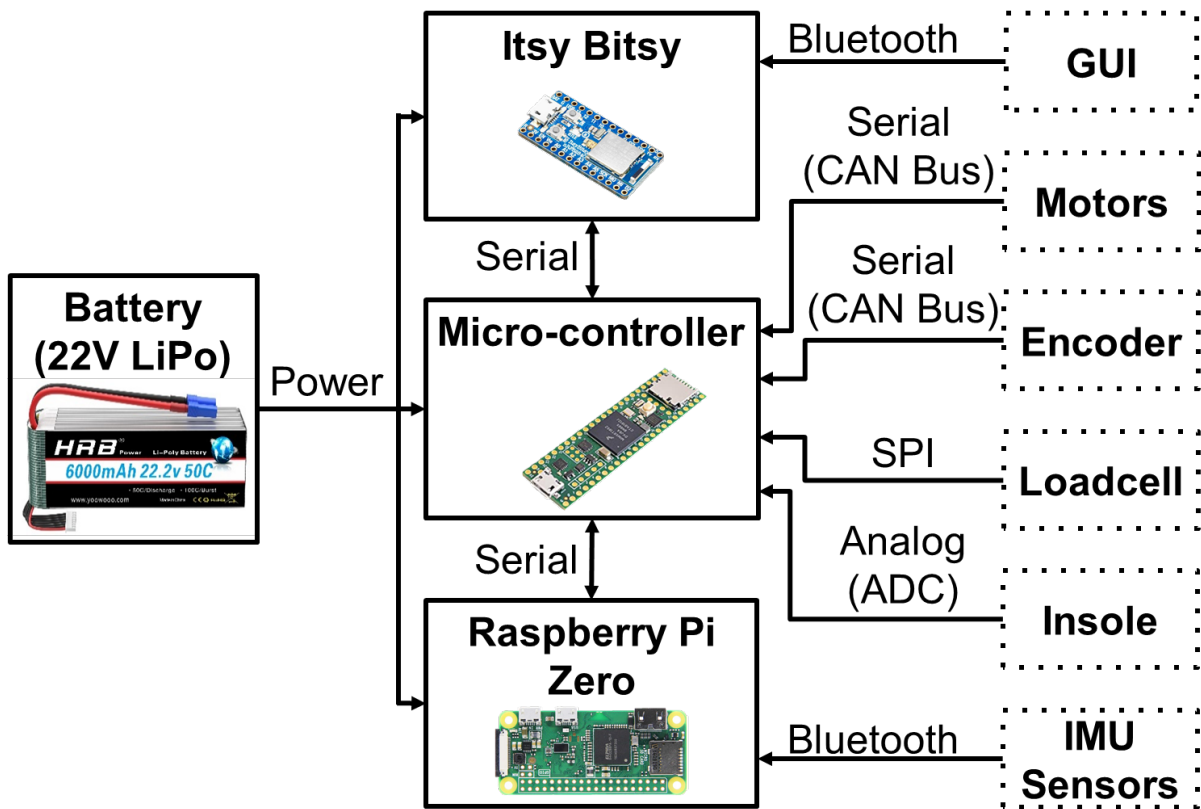


Figure 2.5: Arduino based micro-controller electronic architecture.

gathered by the IMU sensors and the commands given by an operator with a GUI on a PC. All the calculation is done on the micro-controller and not the PC thus reducing the latency of data transmission for the portable exoskeletons. The only communication between the PC and the exoskeleton is through small packets of data transmitted via Bluetooth with a pair of Bluetooth modules, one on the PCB and one at the PC, where only general tuning can be done. The IMU sensors worn by the subject is sent and processed by the Raspberry Pi Zero which can be directly used by the micro-controller. Other ports on the PCB also has an ADC built in to allow for external analog feedback and a voltage regulator for powering the actuator properly with a battery source. Multiple CAN bus terminals are also built in to controller multiple actuators at the same time.

Our compact electronics architecture's simplicity allows the use of inexpensive over the counter parts thus lowering the cost while still be robust and adaptable to different types of exoskeleton design requirements. The lack of required wires and cables also makes the user more comfortable. The overall size of the control box itself is small which can be seen in Figure 2.4. The majority of the mass is in the battery making it lighter and more comfortable for the wearer. Depending on the design requirements, the architecture's modular design allows certain parts to be added or removed as needed.

### **2.1.3 Small Factor Form Computer with Base Architecture (JPU or Raspberry Pi**

To implement a more complex high level control design, the base configuration using just the micro-controller may be difficult and complex. Thus using a small form factor computer, such as a JPU or Raspberry Pi, would be easier to implement since it uses a more traditional programming paradigm. The communication schematic using the JPU as an example is described in Figure 2.6. The JPU is able to run machine learning for the

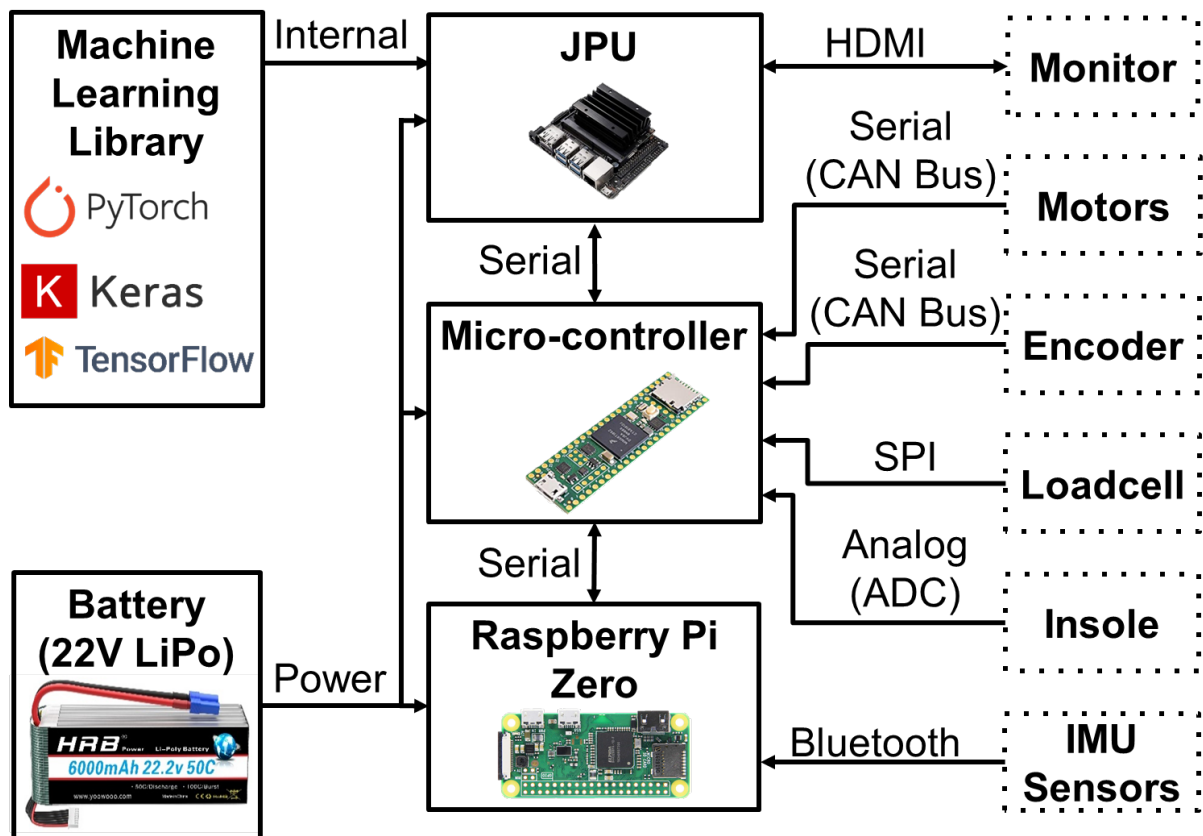


Figure 2.6: Small form factor computer with base electronic architecture.

high-level control while still being small and portable to be used with a portable wearable robot. All the sensor functions and communication method remains the same as in the base architecture with the only difference is that there is no more need to connect to a user control computer via Bluetooth. All the programming can be done on the JPU similar to a normal computer before connecting to the portable system via an Universal Asynchronous Receiver/Transmitter (UART) chip for a serial communication between the JPU and the Teesny micro-controller.

Since both the JPU and Raspberry Pi are smaller than the base electronics box, the overall size increased by the thickness of the type of computer used. Adding just the JPU with the base architecture increase the thickness by roughly 4 cm and increased the weight by 340 g, so when compared to the base architecture the overall mass and size did not change substantially.

#### **2.1.4 Real-Time Machine with Base Architecture (Simulink Real-Time Machine)**

To provide a more robust high-level controller, a real-time machines, such as Simulink Real-Time Machine, can be used in conjunction with the base Arduino architecture. Using Simulink Real-Time Machine as the high-level controller allows for real-time tuning during operation that can make tuning exoskeletons to suit individuals much faster than stopping when a change is needed. The schematic using this configuration is described in Figure 2.7. The Simulink Real-Time Machine communicates with the microcontroller via UART chip that allows for serial communication between the micro-controller and Simulink Real-Time Machine to read and write data packages.

Simulink Real-Time Machine works with MatLab/Simulink programming environment with Simulink uses a graphical block diagram programming that can easily model dynamic

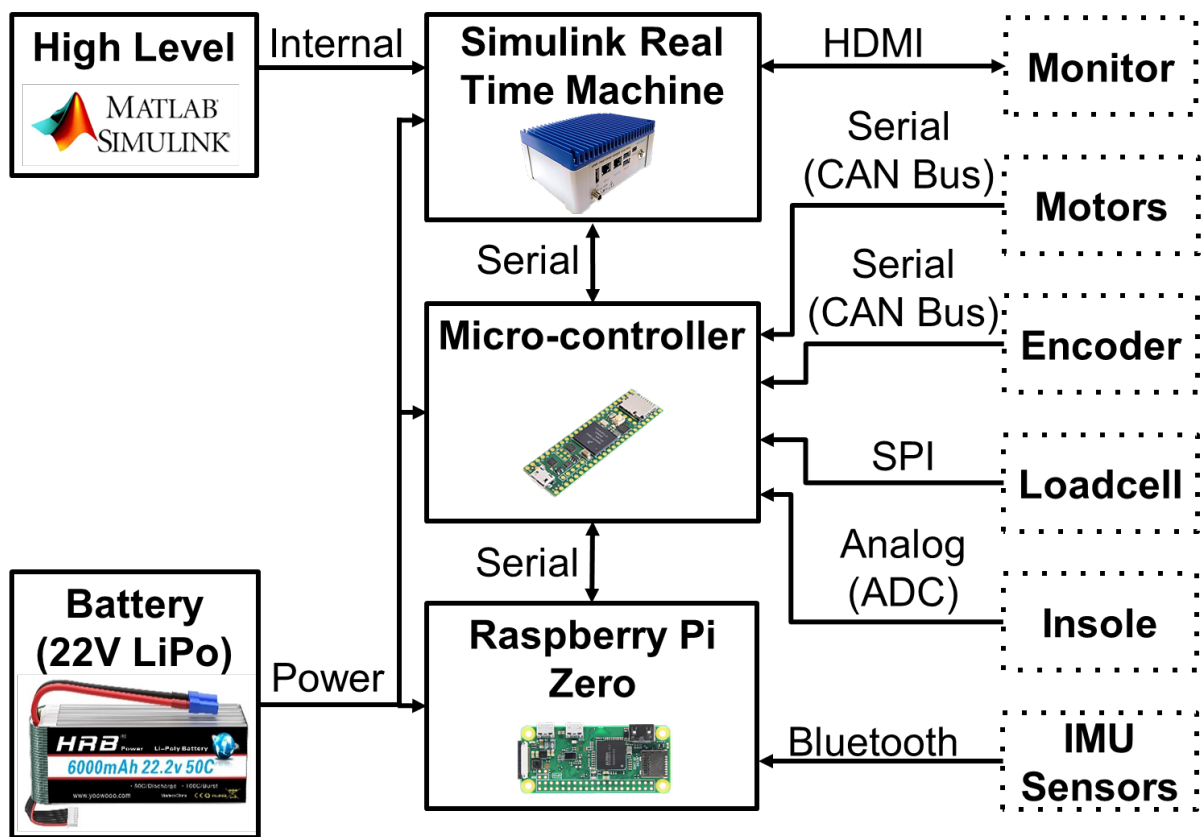


Figure 2.7: Real time machine with base architecture.

systems making it suitable for dynamic model based high-level control for exoskeletons. The sensor data used by high-control can also be used by Simulink Real-Time Machine. The microcontroller in the base architecture directly reads the data from the sensors can also be transmitted to the Simulink Real-Time Machine to be used via the same UART wires without any loss of transmission speed.

The overall weight with this configuration is around 1300g. This makes the real-time machine with base architecture configuration the heaviest configuration when compared to the previous configurations. The overall size of the configuration is around 12.6cm by 16.5cm by 14.2cm making it also the bulkiest configuration. However, it can also be more robust when compared to the other configurations making this a design trade-off between wearable comfort and controller efficiency.

## 2.2 Sensors

Sensors are used by robotic systems to interact with their environment, so they are essential in any types of robotic systems. For industrial manufacturing robots may only require sensors to tell the robot where they are in the space they are occupying, but for wearable robots, more types of sensor may be needed since the human is a part of the system instead of just an external variable. Using our electronics architecture, our wearable robots are able to connect to inertial measurement units (IMUs), insole footswitches, loadcell torque sensors, built in motor encoders, and built in current encoders where their communication protocol and purpose is described in Figure 2.8

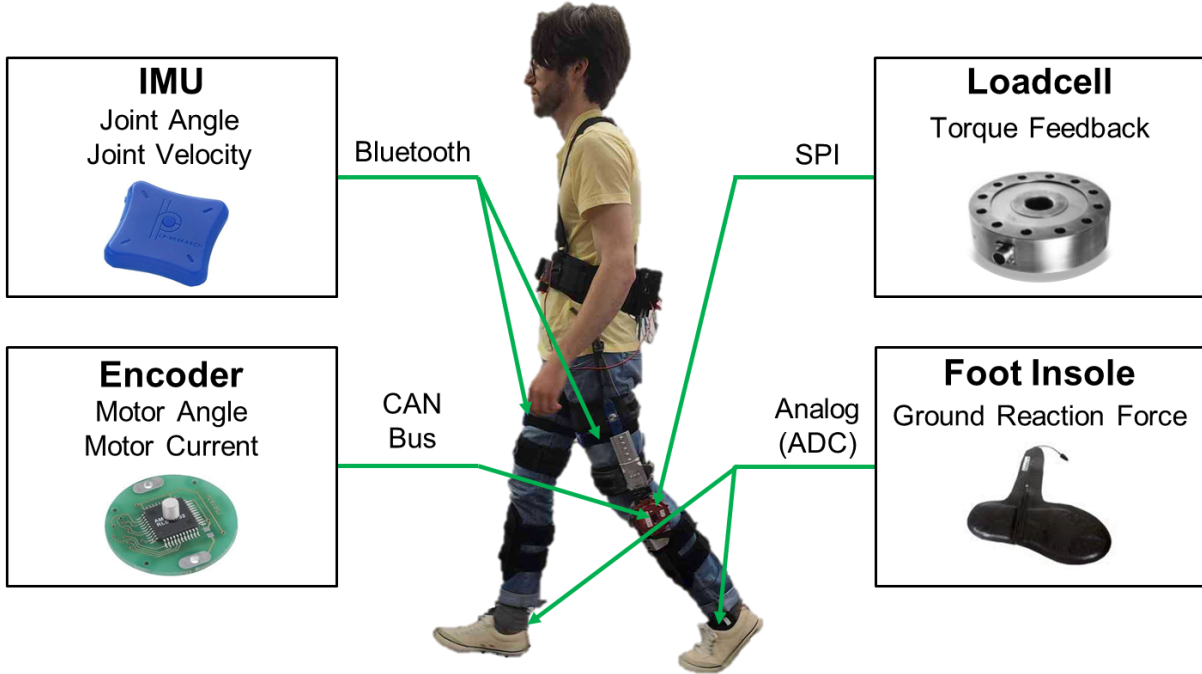


Figure 2.8: All wearable sensor used for wearable robotic system. All sensors can be connected concurrently with our electronics architecture.

### 2.2.1 Inertial Measurement Unit

The inertial measurement units (IMUs) can be worn on the body using velcro straps so the exoskeleton can be portable. We attached two wireless IMU sensors on the thigh and shank of each leg to measure biological knee angle during walking. The IMUs connect with the micro-controller through Bluetooth. To connect each IMU, a local hotspot created by the custom Raspberry Pi Zero image would be accessed to the GUI that connect the IMUs to start sending data. The data received from the Raspberry Pi Zero is directly sent to the micro-controller via 100 Hz serial communication. The connection itself between the Raspberry Pi Zero and micro-controller is physically

The IMUs are of 3-axes. Thus to measure the biological joint angles, Euler transformation calculations are done in the code to obtain the angles from the axes from the thigh and the

shank. The main benefit of using these IMUs is its portability and its wireless capabilities. With many types of sensors available, the number of hard wire connections are needed; however, a large amount of wires and cables makes it difficult and uncomfortable for the user. Which is why the wireless IMUs we used is important as it is able to accurately measure the joint angle quickly without the need for extra wires.

### **2.2.2 Footswitch**

The footswitch sensor is in the form of removable insoles worn inside the user's shoes and is used to measure the ground reaction force (GRF). The footswitch can communicate and send sensor reading with the base PCB through low voltage analog signals. There are two ground common wires and four signal wires that is connected to the micro-controller's analog input pins that reads the force and pressure where each signal wires is connected to a certain areas in the footswitch insole to differentiate the analog readings. All the wires from the footswitch are contained within a single micro-USB cable that can be connected to headers on the PCB that has the necessary connections to the micro-controller, so at most only two cables are need to connect the footswitch sensors making it more comfortable for the wearer.

Since the profile of the GRF can be used to determine the different phases during a gait cycle as well as the user's intention Lerner et al. (2017a), the footswitch sensors is a lightweight method for controlling lower limb exoskeletons. The footswitch sensor does not require any special calibration and can be used immediately with the only requirement is the size of the footswitch should fit the wearer. Improperly fitted footswitch could cause inaccurate readings since the pressure on the foot from the ground may be misaligned with the position on the footswitch or the footswitch could also shift from being too small. For upper-limb exoskeletons where footswitch sensors would not be as useful, the sensors do

not to connected to the PCB and the port can be left open without any alteration.

### 2.2.3 Torque Sensor

A loadcell is used to measure the actual torque at the joint due to the biological knee moment and the exoskeleton. To ensure the loadcell is reading the correct torque, it is mounted in parallel with the actuator thus can directly measure the torque without needing additional calculations to account for the displacement of the loadcell from the actuator and joint. To connect the loadcell, microUSB headers are installed on the custom PCB board near the motor ports. The Serial Peripheral Interface (SPI) connections the loadcell communicate with the on board micro-controller is are already made in the PCB ensuring reliable connection.

Including the loadcell into the system allows for a closed-loop torque control that is used to accurately track the reference proportional torque profile provided by the mid-level controller. Loadcell needs to be calibrated before using. Calibration is done by applying a known torque on the loadcell which can be done using simple weights or instrumented torque wrenches and adjusting the gains so the readout matches the expected torque applied.

### 2.2.4 Built-in Sensor in Actuator: Encoder + Current

A quasi-direct drive (QDD) actuator used for all the exoskeletons are smart actuators with angle and current encoder built in which simplifies the overall exoskeleton designs. The encoders is able to measure the motor's angle relative to the starting position as well as the current the motor draws during operation. The electronics architecture setup allows the built in encoder to communicate with micro-controller through the same motor cable. The motor cable itself contains the power lines for the actuator as well as CAN wires to control

the actuator. The measurements from the built in encoder is also transmitted using the CAN bus. Since the actuator can be connected through a single cable, it makes our exoskeleton more portable as more cables can get tangled easily making the user less dexterous and mobile.

To read the measurements from the encoders, an 8-bit command signal can be sent through the CAN bus to read sensor data. No further steps are needed to begin using the encoders. Thus the encoder can be directly integrated into a motor position and current control by sending a read command to the encoder.

## 2.3 Control

Exoskeletons typically uses a high-level controller and low-level controller as shown in Figure 2.9. The high level controller usually uses the biological signals (such as human joint angle, gait cycle, muscle signal) measured by sensors (such as IMU, insole and EMG) as the input to generate the appropriate reference signals as the output. Depending on what is needed by the low-level controller depending on the control framework, the reference signals generated can be torque, current, position, speed, impedance and admittance. Yu et al. (2023); Zhang et al. (2017) The goal of low-level controller is to drive the actuator of exoskeletons as accurately as possible using the reference signal generated by the high-level controller.

### 2.3.1 Torque Control

Wearable robots like exoskeletons assist the wearer by providing an additional torque or force to the wearer. For this reason, controlling the timing and amount of torque the exoskeleton provides is desired. The adopted torque control method can be seen in Figure 2.9

A. As described in the figure, torque control requires an external sensors, i.e., torque sensors, to detect the human and robot interaction torque and to provide a feedback signal to the robot to ensure the accuracy and safety of control. Thus, torque control is the wearable robot's most common low-level control method.

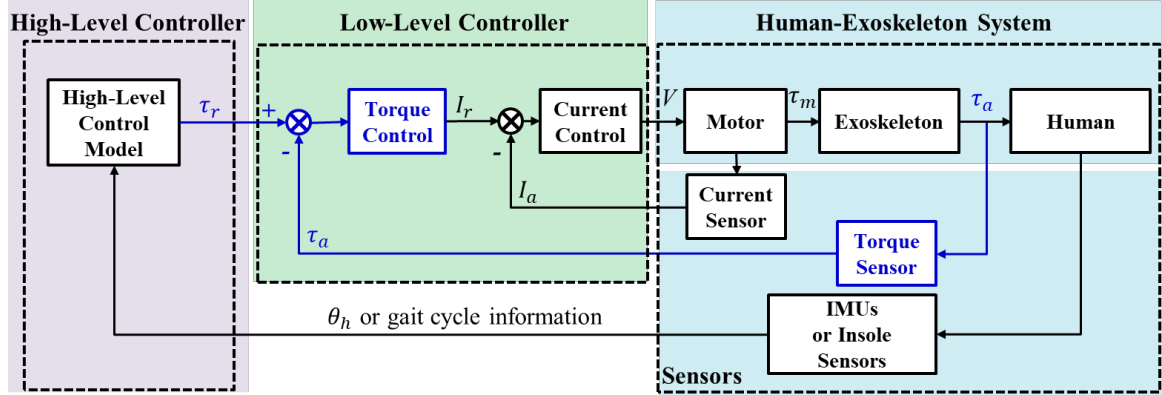
### **2.3.2 Current Control**

Current control and position control generally only need the embedded sensors (current sensor and encoder) already inside the smart actuator. Current control itself is similar to torque control as the major difference is removing external signal feedback making it equivalent to open-loop control. The control method can be seen in Figure 2.9 B. The main benefit of current control is its simplicity since it only requires the current sensor that is already included in the smart actuator without any further changes or calculations. The biggest drawback with current control is that the tracking accuracy comparing the actual output with the reference command is not guaranteed unlike torque control.

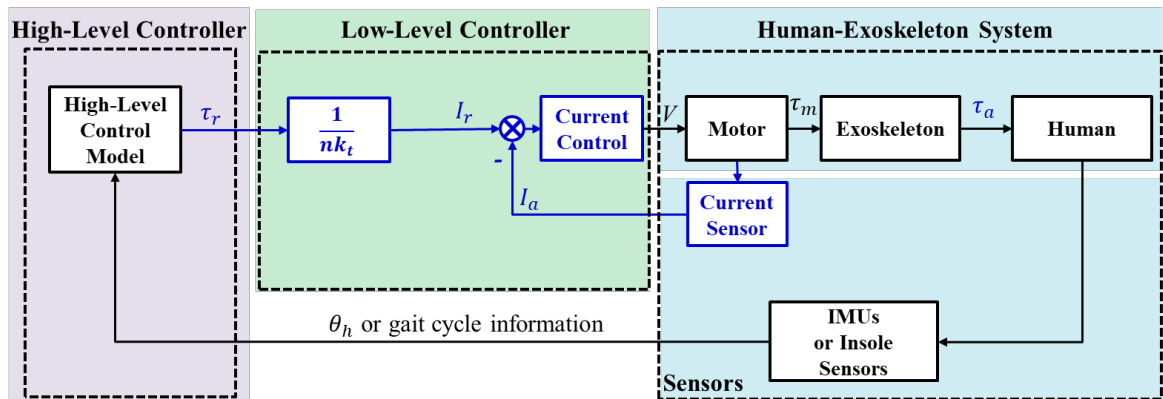
### **2.3.3 Position Control**

The control method for position control can be seen in Figure 2.9 C. Position control generally follows fixed position trajectory in space as the reference signal is the exact joint angle the wearable robot should be. For exoskeletons this may force users to move their limbs according to a fixed position trajectory. Therefore, the position control is not complaint to the user's input changes and sudden environmental changes, so its use is limited to stable periodic tasks. For prostheses, however, position control can be very useful. Since instead of providing an assistive torque, prostheses are used for support during locomotion so controlling it using the intended position is a good fit.

### A.) Torque Control



### B.) Current Control



### C.) Position Control

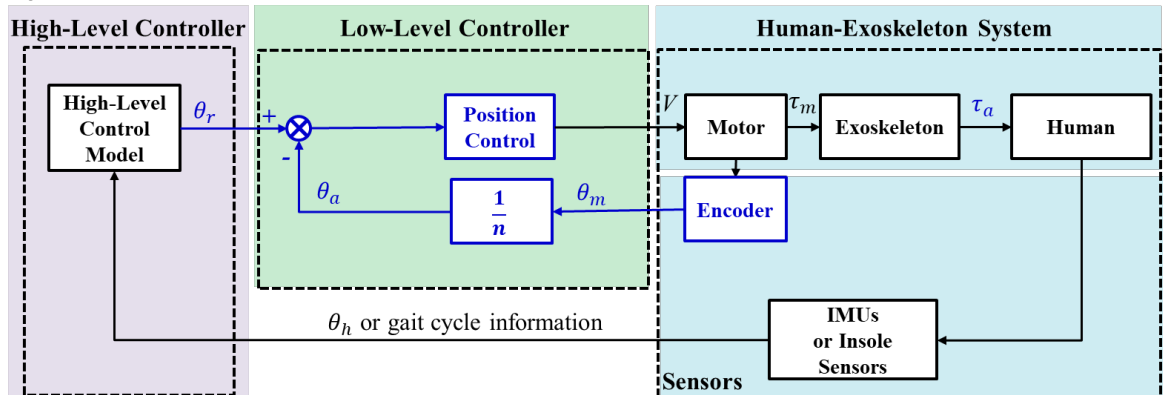


Figure 2.9: Three different types of control methods (torque, current, and position) that is commonly used for wearable robots.

### 2.3.4 Experimental Results

To evaluate the effectiveness of each type of control method, a QDD actuator was mounted on a benchtop setup that holds the QDD actuator's stator in place while the rotor is free to rotate. Each type of method uses a 1 hertz wave signal as the reference.

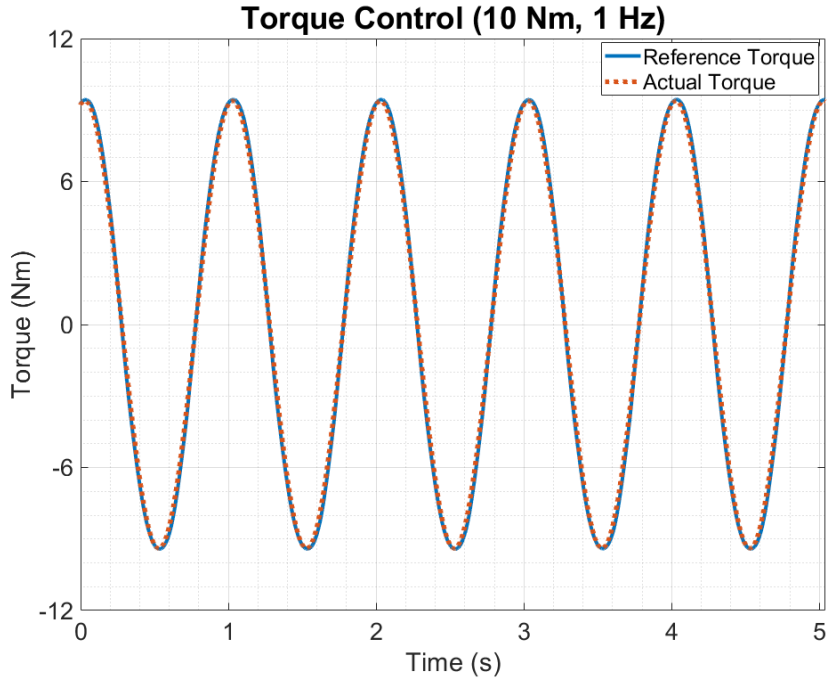


Figure 2.10: Torque tracking of a 1 hertz wave at a magnitude of 10Nm as the reference signal where the RMSE is 0.005 Nm.

For wearable robotics like exoskeletons, its purpose is to provide a torque at the proper moment in time, so a torque tracking experiment is done to evaluate the accuracy between the command signal and the output torque. With the bench-top setup, a 1 hertz wave reference signal with an amplitude of 10 Nm was sent to the QDD actuator. The result of the torque tracking experiment can be seen in Figure 2.10. The RMSE of the experiment is approximately 0.005 Nm. The percent difference from the RMSE and the peak torque was

0.05°. These results prove the high torque accuracy of the QDD actuators and loadcell with our electronics architecture.

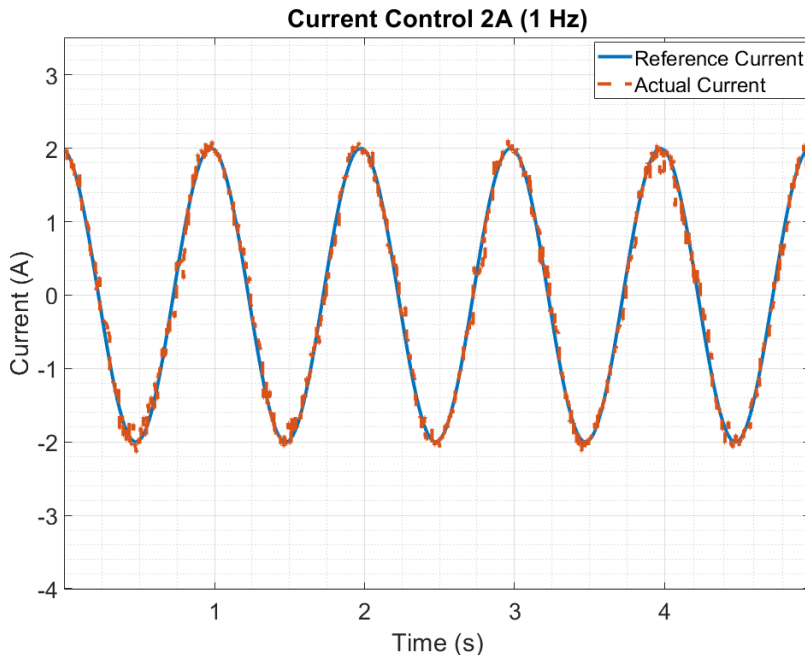


Figure 2.11: Motor angle tracking of a 1 hertz wave as the reference signal where the RMSE is 0.0025 A.

Evaluating the QDD actuator with the electronics architecture using the current control method was also done. Along with position control, current control also uses the built-in encoder in the QDD actuator itself, so a the current draw measurement from the encoder can be directly measured using the same CAN cable. Similar experiment was done, but the actuator is driven by a 1 Hz wave reference signal with a 2 A amplitude. The results can be seen in Figure 2.11. The RMSE was only 0.0025 A, so the percent difference between the error and peak current was 0.125%. Current control had the least error in tracking is due to how simple the low level control scheme was with the built-in encoder giving a direct measurement of current draw.

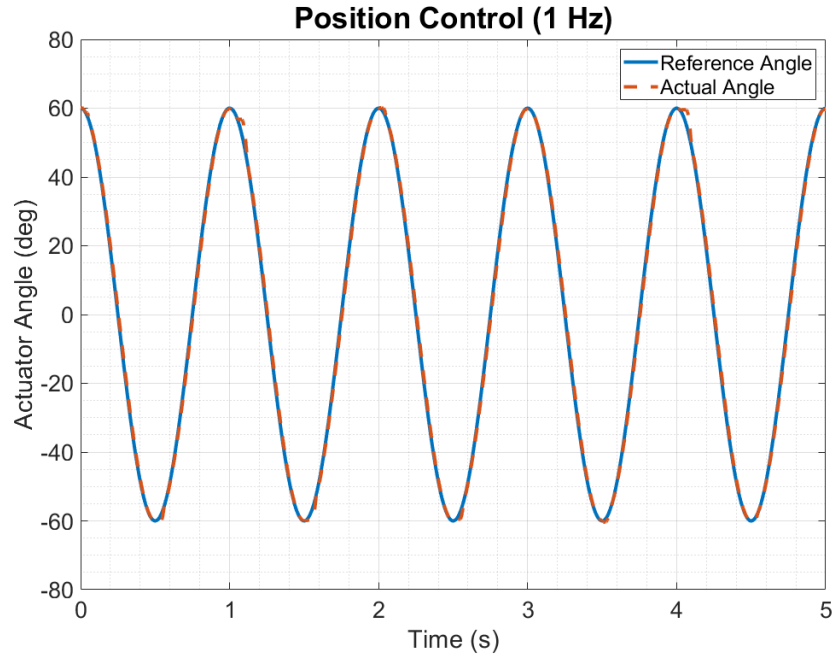


Figure 2.12: Motor angle tracking of a 1 hertz wave as the reference signal where the RMSE is  $0.1312^\circ$ .

For the position control, the reference signal is a 1 hertz wave signal with an amplitude of  $60^\circ$ , and the results can be seen in Figure 2.12. The root mean square error (RMSE) between the reference and actual measurement represent the variation between the reference and actual measurement, so a smaller RMSE represent a more accurate tracking. The position control experiment results in a RMSE of  $0.1312^\circ$ , and compared the peak angle of  $60^\circ$ , the difference was  $0.219^\circ$ . This supports the accuracy of using the built-in encoder with our electronics architecture.

### 2.3.5 Graphical User Interface

An interface is not just designed for the communication between the user and robot. A graphical user interface (GUI) can also serve as a means of communication between the engineer, clinician, and user to ensure the proper use of the wearable robot. By controlling

the states of the wearable robot and being able to record valuable data wirelessly, a GUI has become a necessity with wearable robots. Tucker et al. (2020) We developed a GUI (MatLab) that is able to tune and control the exoskeletons via Bluetooth while also being able to record data as described in Figure 2.13. With the base code in the micro-controller, the GUI is able to control the exoskeleton without the need to constantly upload new parameters or settings. The main tuning parameters regardless of the control model used is the type of assistance provided, extension or flexion, magnitude, saturation, shift, and duration. The magnitude controls the peak torque the exoskeleton will provide, the saturation controls how quickly the torque reaches the peak, the shift controls the timing of the assistive torque, and the duration controls how long the pulse of torque would be provided. Depending on the model, the effect of these parameters would vary. The outputs from the control can be seen in the four plots in the middle of the GUI. The joint angle measured using the wearable IMUs on the thighs while the current command and torques are measured by the actuator's encoders send using the CAN buses.

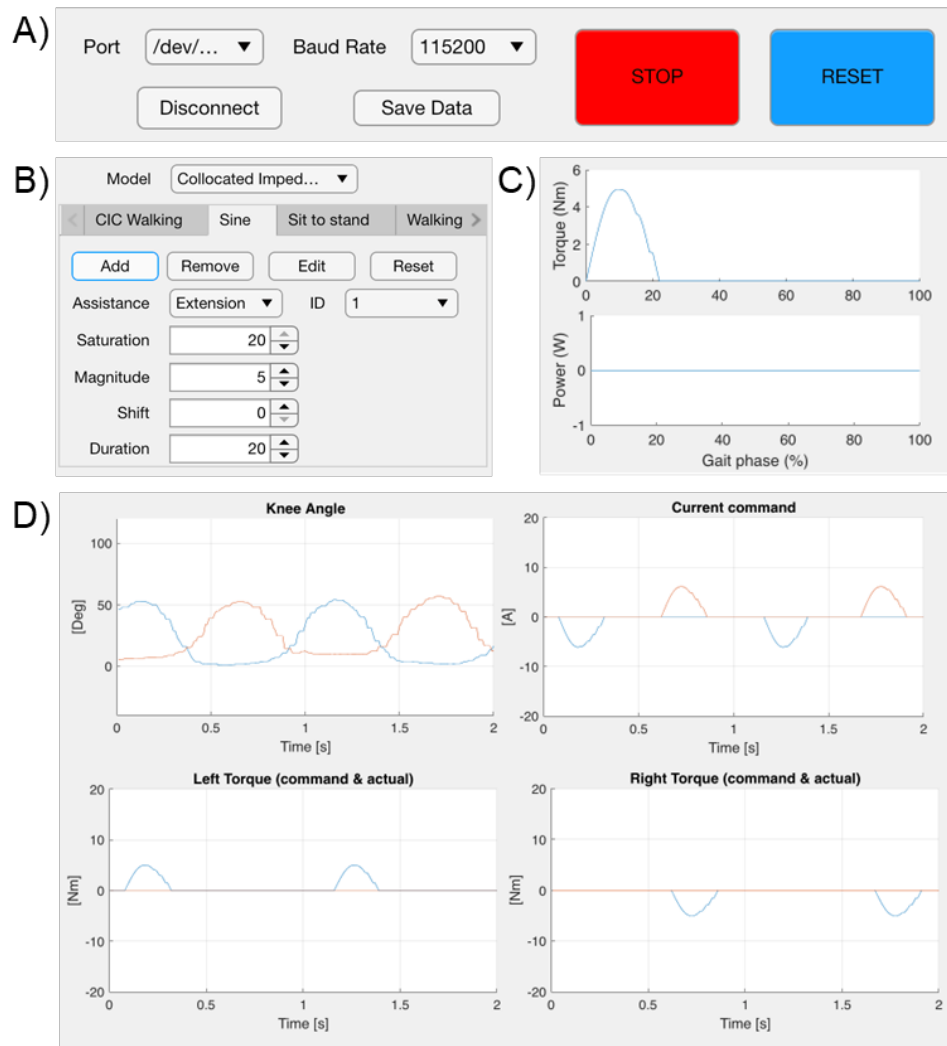
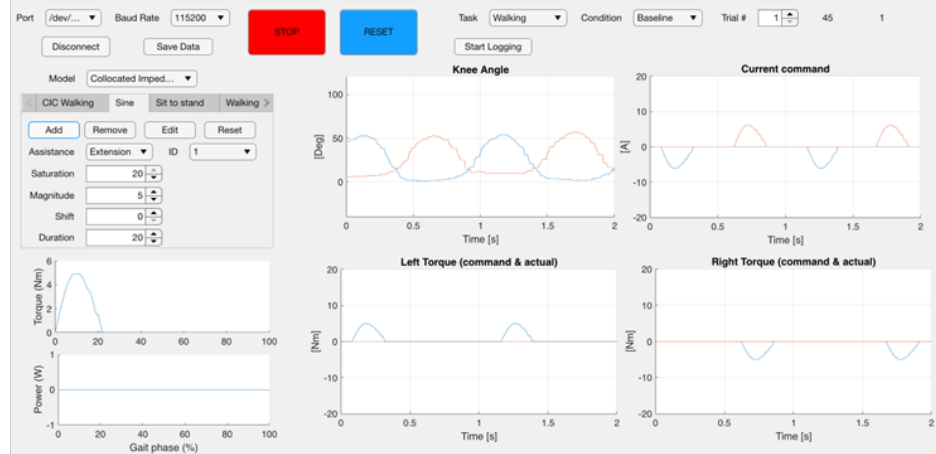


Figure 2.13: Functions of the custom graphical user interface. It is able to set the Bluetooth connection ports as well as to control the estimation model and tuning. The command and sensor data is also plotted in the GUI

## CHAPTER

### 3

# RIGID WEARABLE ROBOT - KNEE EXOSKELETON

The main advantage of a rigid exoskeleton is the force transmission efficiency when compared to soft exoskeletons. Since rigid exoskeletons are made of rigid linkages and joints, the dissipation of force being transmitted due to deformation and translation of the exoskeleton are small as opposed to soft exoskeletons where the assistive force would cause unwanted deformation or translation during operation. Due to the design requirements, the rigid exoskeleton paradigm was selected and a new generation of rigid knee exoskeleton was designed.

The knee joint is a key joint that helps with balance and mobility during the gait cycle where key point is the transition between the stance and swing phase. Huang et al. (2022) The knee also undergo many repetitive loading tasks, especially in construction work, due to constant getting up and down from kneeling. Chen et al. (2021) The designed knee exoskeleton is composed of one actuator per leg, support frames for the thigh and shank, and a waist-mount system. The actuator transfers torque through the support frames to the user's knee joint. The support frames each fasten to the corresponding limb segment through a cuff with adjustable Velcro straps. An adjustable pre-tensioned elastic strap connects the support frames to a sturdy waist band that is also supported by shoulder straps, which prevents the exoskeleton migrating down the legs and causing joint misalignment in the sagittal plane. A single-hinge mechanism located on the shank support frame reduces the joint misalignment in the frontal plane. The 3D printed cuffs and soft, textile straps are modular and adjustable to ensure a good fit for a large range of physiques. These features together provide a comfortable experience for the wearer and reduce misalignment during torque assistance.

### 3.1 Knee Exoskeleton Development

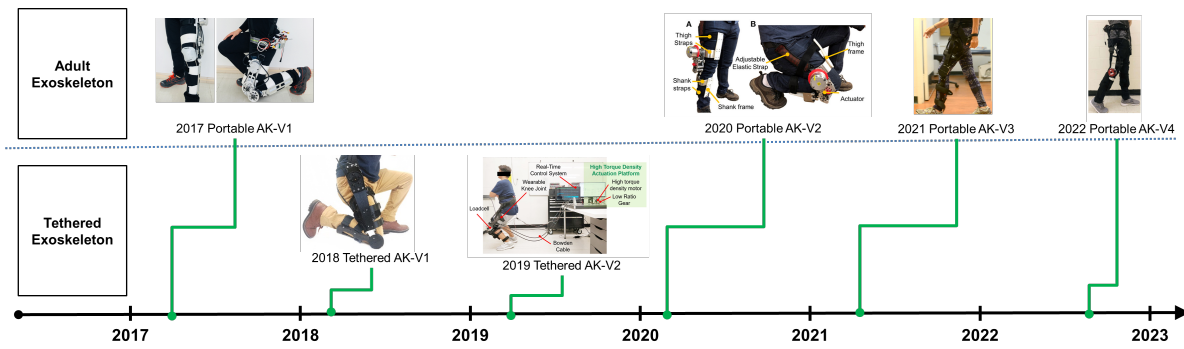


Figure 3.1: Timeline showing the evolution of our lab's knee exoskeletons.

Previous generations of knee exoskeletons have been developed by the lab. Figure 3.1 shows the generations of both tethered and portable knee exoskeletons that have been designed for both adults and pediatric purposes. Both tethered and untethered versions of the knee exoskeleton have been developed. As the knee exoskeleton evolves, many features have been added or removed depending the design requirements and engineering trade-off decisions. Such as for the 2018 Portable AK-V2 exoskeleton, it is a bio-inspired knee exoskeleton that better matches the actual actuation in the knee, but was a lot bulkier when compared to newer version. Yu et al. (2022) To design a new version of knee exoskeleton, the latest exoskeleton was used as the starting point. The CAD model of the latest knee exoskeleton can be seen in Figure 3.2

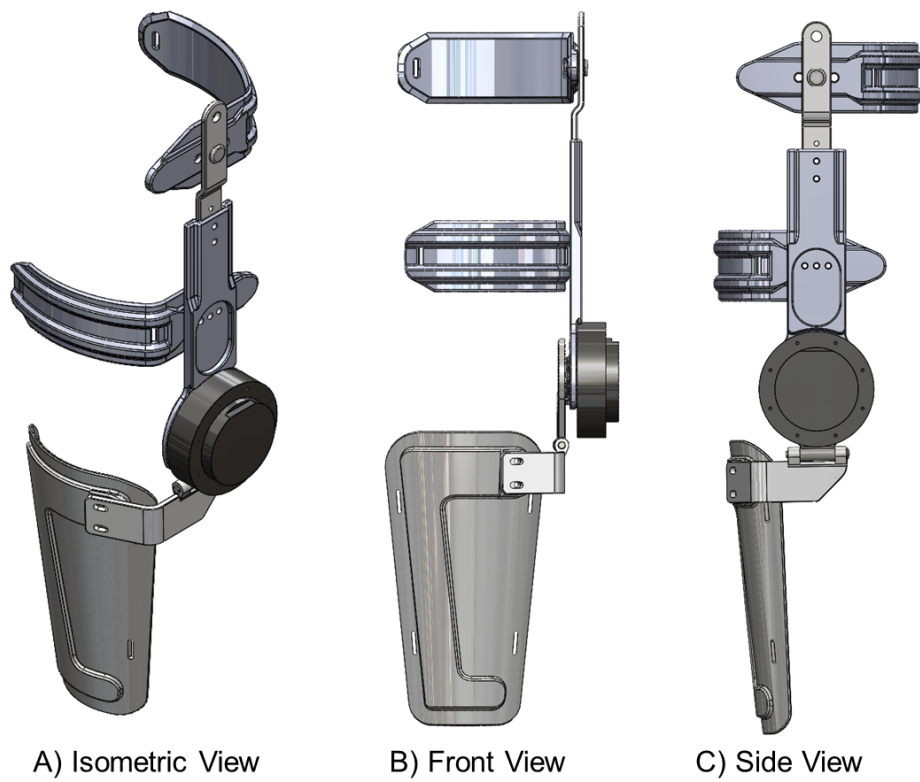


Figure 3.2: CAD model of the latest knee exoskeleton.

For the new generation of knee exoskeleton, the mechanical design goals are to:

1. Reduce the overall mass of the knee exoskeleton.
2. Smaller overall size to allow for ground kneeling to stand.
3. Improve the wearable straps' comfort.

An overview comparison of the latest generation vs the newly designed exoskeleton is described in Table 3.1

Table 3.1: Comparison of Knee Exoskeleton

	Current Version	New Version
Total Mass (kg)	3.84	3.28
Total Length (mm)	570	434
Peak Torque (Nm)	20	36
Voltage (V)	24	24
Battery Life (hr)	2.0	2.5

## 3.2 Actuation

For the exoskeleton to provide an assistance torque to the wearer, an actuator is needed. There are many types of actuators available with many ways of supplying force, such as hydraulic, pneumatic, and electromagnetic, where each has its own drawbacks and functionalities. Both hydraulic and pneumatic actuation requires a tethered pump to provide force, so they are not good choices for a portable exoskeleton system. For the knee exoskeleton designed, an electromagnetic actuator is used. Common motors used are brushless direct current (BLDC) motors. However, a challenge with BLDC motors is that their torque

are relatively low but can provide a high angular velocity. Most actuator designs uses the BLDC motor as a base and uses a high gear ratio to both reduce the rotational speed that would be safe for humans while providing a higher torque so that the torque supplied would be significant when compared to the biological torques produced from the wearer's muscles. A high gear ratio has its own drawbacks however, a higher gear ratio equates to a higher inertia in the actuator. This not only makes the actuator heavier, but it also makes it harder to turn the actuator. Having a compliant, or backdrivable, actuator is beneficial for wearable robotics because, a properly exoskeleton should not dictate or hinder the wearer's natural movements but rather work in parallel with the wearer. Witte and Collins (2020)

### **3.2.1 Quasi Direct Drive Actuator**

Quasi direct drive actuators (QDD actuators) are also known as proprioceptive actuator and pancake motors due to their flat shape. They are characterized by their high torque density, energy efficiency, and backdrivability. Wensing et al. (2017)

As stated in their name, QDD actuators have relatively low gear ratio, so that the output of the actuator acts similar to a direct drive actuator. Due to the low gear ratio, the inertia is also relatively low which means a low amount of torque is needed to turn against the actuator. This disadvantage is solved by the high torque density motor that has been geometrically optimized. Wensing et al. (2017)

Also due to the low gear ratio, the overall inertia of the actuator has also been reduced. Excessive gears and other mechanical components can lead to heat through friction. By simplifying their mechanical complexity, the energy efficiency of QDD actuators are also improved.

When considering the design requirements of a wearable robot, QDD actuators have many qualities that are suitable solutions to the design challenges. One of the challenges

was the backdrivability also the compliance of the actuator. Having a low backdrivable motor means that the motor have difficulties turning from an external force. In many applications this would be very beneficial since the motion and control of the actuator will be more precise. For wearable robotics, however, humans are working with robots and is a major part in their control scheme. Having an actuator with low backdrivability will cause the entire system to be driven by the robot and not allow any natural movements from the wearer. Thus, a compliant actuator with high backdrivability is ideal for wearable robotic application. This was why a QDD actuator was chosen, their relatively low gear ratio with their high torque density motor allow for a relatively higher torque than conventional BLDC motor while still being compliant to ensure the wearer's safety.

In many cases, the torque supplied for wearable robotics may not need to be as high as industrial manufacturing robots. Applying extremely high torque can cause severe damage to the wearer which is why in the case for exoskeletons only a fraction of the normal biological torque should be applied to the wearer. The biological knee moment for a person will vary based on the person's body type, but for normal daily activities the biological knee flexion moment average around 3.16% BWm (Body weight in Newtons x meter) and the extension moment would average around 0.44% BWm. Kutzner et al. (2010) The QDD actuators used can reach a nominal torque around 14 Nm nominal torque and a 20 Nm peak torque. Yu et al. (2020), Huang et al. (2022)

With the QDD actuator is also composed of a torque sensor and embedded system for low-level control. The custom torque sensor transfers torque loads from the actuator output stage to the shank support frame through bolted connections on each end. The sensor is rated for torques up to  $\pm 40$  Nm with a resolution of 0.1 Nm. The torque range and backdrivable torque of actuator makes it suitable for the knee exoskeleton.

### 3.2.2 Actuator Selection

To meet the mechanical design goals of reducing the overall exoskeleton weight and ground clearance when kneeling, a lighter QDD actuator with a smaller diameter was selected. To compensate, for the smaller diameter the new actuator is a bit thicker than the previous actuator. A comparison of the specifications of the previous actuator and the new actuator is described in Table 3.2.

Table 3.2: Comparison of Actuator

	<b>Current Actuator</b>	<b>New Actuator</b>
Voltage (V)	24 - 48	24 - 48
Diameter (mm)	98	76
Thickness (mm)	42	58.5
Gear Ratio	9:1	36:1
Mass (kg)	630	600
Rated Torque (Nm)	9	18
Peak Torque (Nm)	27	54
Speed (rad/s)	17	7

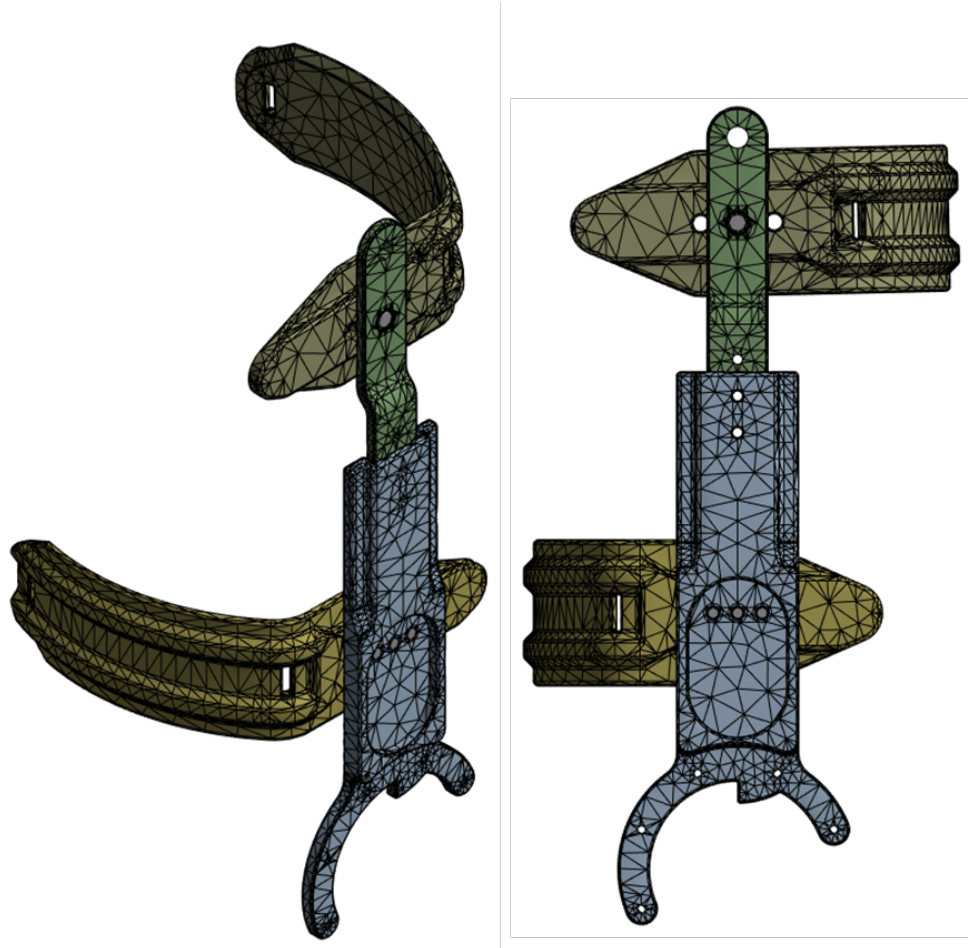
As the thickness of the actuator has less impact when considering the ground clearance when kneeling compared to the overall diameter, a 22 mm reduction in the diameter compared to an 16.5 mm increase in thickness makes the new actuator to be better suited to the kneeling design of the updated exoskeleton. The only other specification that changed is the gear ratio. At 36:1 gear reduction, the output torque can be much higher compared to a 9:1 gear reduction to provide a wider range of magnitude for the output torque.

## 3.3 Mechanical Design Improvements

### 3.3.1 Finite Element Analysis

Ideally, a rigid exoskeleton would need to be strong enough to support the torque provided by the actuator as well as its own mass when worn while not increasing the metabolic cost of the wearer without the exoskeleton on and without altering the wearer's natural movement and intent. Realistically, however, an exoskeleton is an additional mass for the wearer since it is a physical dynamic system, so its extra would increase the metabolic cost and alter the natural kinematics of the wearer. For any type of exoskeleton to be beneficial, it should be able to provide assistive or rehabilitative effect on the user while also overcoming the mass penalty of the exoskeleton itself. Finite Element Analysis (FEA) can be used to help optimize the mass of exoskeletons. FEA was used to calculate the stresses in the rigid structure for the current generation of knee exoskeleton. By finding the areas where stress concentrate and areas where there is little stress, the topology of the exoskeleton can be alter to where the mass and volume of the exoskeleton can be reduced. For the knee exoskeleton, the thigh bar is the main contributor to the overall mass of the exoskeleton, so it was the main focus for FEA simulation.

The key principle of FEA to find the stresses in a rigid body's topology is to discretize the volumes in the 3D model into a mesh of cells. The generated mesh can be seen in Figure 3.3 To calculate the stress of the structure, each cell in the body is calculated with the equation for stress (Eqn. 3.1) as a matrix where each cell is an element in the matrix. To solve the matrix equation, boundary conditions are set in certain cells to represent its behaviour, such as the applied force or external supports, that is determined by how the simulation is setup. The boundary conditions for the thigh bar was setup by how the exoskeleton is worn.



Statistics	
<input type="checkbox"/> Nodes	47013
<input type="checkbox"/> Elements	24734

Figure 3.3: Generated mesh for FEA with 24734 tetrahedron elements for calculation.

$$[\sigma] = \frac{[F]}{[A]}$$

$$\boldsymbol{\sigma} = \begin{bmatrix} \sigma_{11} & \dots & \sigma_{1n} \\ \vdots & \ddots & \vdots \\ \sigma_{m1} & \dots & \sigma_{mn} \end{bmatrix} F = \begin{bmatrix} F_{11} & \dots & F_{1n} \\ \vdots & \ddots & \vdots \\ F_{m1} & \dots & F_{mn} \end{bmatrix} A = \begin{bmatrix} A_{11} & \dots & A_{1n} \\ \vdots & \ddots & \vdots \\ A_{m1} & \dots & A_{mn} \end{bmatrix} \quad (3.1)$$

When wearing the exoskeleton, the thigh bar is held in place using two 3D printed braces using carbon fiber (Markforged Mark Two Onyx™). The proximal brace is on the posterior side of the thigh while the distal brace is on the anterior side of the thigh. This configuration fixes the thigh bar from rotating and moving in all directions but axially with the thigh, so the thigh bar would slide down over time. To prevent this translation, an elastic band is hooked on the tip of the thigh bar to the waist band thus preventing the thigh bar from sliding.

This setup is replicated in ANSYS to run the structural FEA to find the maximum stress and deformation at the smallest mass. The FEA simulation setup is described in Figure 3.4. The thigh braces are set as displacement supports so that the only direction the brace can move is in the z-axis since just using the braces means the thigh bar would slide down the thigh but cannot move in any other directions. The cylinder support where the elastic band is holding the thigh bar has the only direction free is the tangent direction. This represents how the elastic band is able to support the thigh bar from moving forward or sideways but not rotating around the elastic band. Screws are used to connect the braces to the thigh bar, and this was also represented in the analysis using a pretension screw force in the areas screws are used. A ramping moment to 20 Nm was used at where the actuator is positioned as 20 Nm was peak torque measured from previous works from the lab. Huang et al. (2022), Yu et al. (2020), Zhu et al. (2022)

The FEA results are described in Figure 3.5. The original design had the largest mass

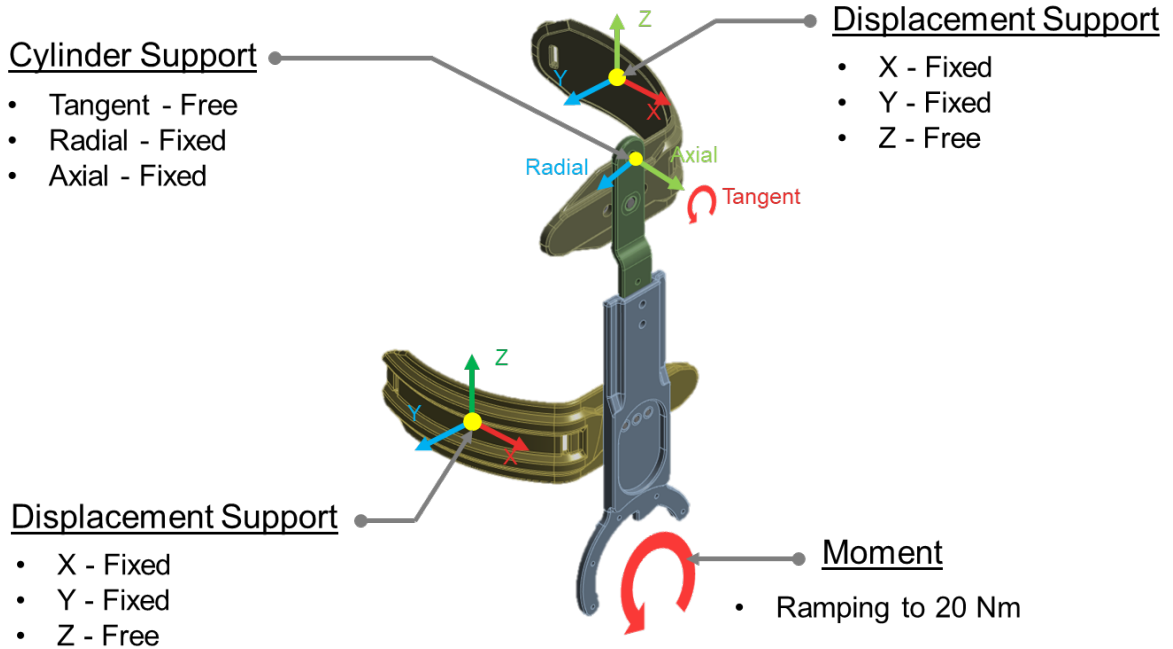


Figure 3.4: FEA setup for the thigh bar for the knee exoskeleton.

which was expected with a maximum stress of 54.128 MPa where the flange connecting the actuator to the main body of the thigh bar, so to remove the stress concentration the radius at that corners are increased. The first version of the thigh bar tested was able to reduce the maximum deformation while keeping the stress similar to the original, but it would be difficult to manufacture due to the irregular cut in the bar. Thus, a second version was made that both remove the excess mass using a hole lattice structure, reducing the thickness of the bar, and increasing the fillet radius at the flange corners. The max deformation was slightly higher than the first version but still lower than the original while having a lower maximum stress compared to previous designs. The mass for the second version was also much lower. A third version was also made using carbon fiber instead of aluminum alloy. The overall mass definitely decreased greatly, but this design was not chosen since it requires the thigh bar to be made with a new material which requires more planning for manufacturing. For

future research, using a 3D printed carbon fiber designed rigid structure could be worth looking into.

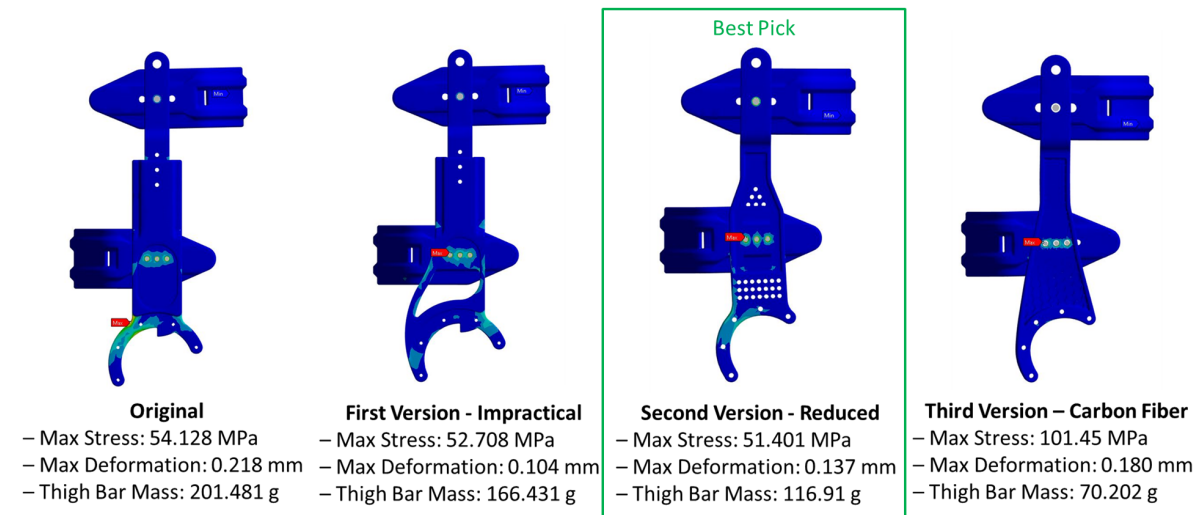


Figure 3.5: FEA of stresses due to 20 Nm actuator on the thigh bar of the knee exoskeleton.

### 3.3.2 Wearable Structure

The wearable structure often appears to be the simplest parts on an exoskeleton, but it is just as important as the mechanical, electrical, and control design. Wearable structure is the interface between the exoskeleton and the wearer, so a properly designed and fitted wearable structure can allow the wearer to feel a more pronounced assistance because wearable structure is the last part the forces from the actuator travels through before reaching the wearer. However, most wearable structures are designed with a specific wearer and is custom made to fit the specific wearer. Bulea et al. (2022) For the wearable structure to fit a wider range of people, a trade off needs to be made where the fit may not be as optimal.

For an exoskeleton's wearable structure to fit a wider range of body types while still

being comfortable for the wearer, lightweight to not incur metabolic penalty, and effectively transfer torque from the actuator. The wearable structure for the knee exoskeleton designed are modular, so the braces and straps are interchangeable which allows for a wider fit range without compromising on the exact fit for the wearer. There are three anchor point for the braces with one brace on the shank and two at the thigh. Each brace is comprised of a 3D printed rigid part made of carbon fiber (Onyx™, MarkForged). The braces can be seen in figure Figure 3.6. The main brace changes are in the shank brace. The length of the shank brace has been greatly reduced, and the connection points have been moved from the top of the brace to the middle of the brace. When the connection point was at the top of the brace, the brace can easily dig into the wearer since the brace itself is long and geometry is uneven at the connection point. With a smaller shank brace and connection point in the middle of the brace, it solved the major problems with the current brace. Another change is in the lower thigh brace where a small slope was added to the interface. Since the thigh can be thought to be similar to a cone where the top of the thigh cone is the base and the thigh at the knee is near the point of the cone. The slope added to the lower thigh brace provides a more ergonomic fit for the wearer. A comparison of the current wearable structure to the updated structure can be seen in Table 3.3.

To secure the 3D printed brace to the wearer, a cloth padding underneath held together with Velcro straps sewn on the padding that comes together allowing the 3D printed brace to change to a different size according to the wearer. Velcro cinch straps are sewn on the padding so that it can be worn on the legs. The length of the Velcro hook pad has also been shortened which can be seen in Figure 3.7. The shortened hook pad allowed for a wider range of fit for the wearable straps. A long hook pad had the problem of not reaching the cotton pad if the wearer required a larger fit. Just by using a shorter hook pad, the strap fit can easily be seen since the shorter hook pad can easily reach the cotton pad when looping through plastic hoop.

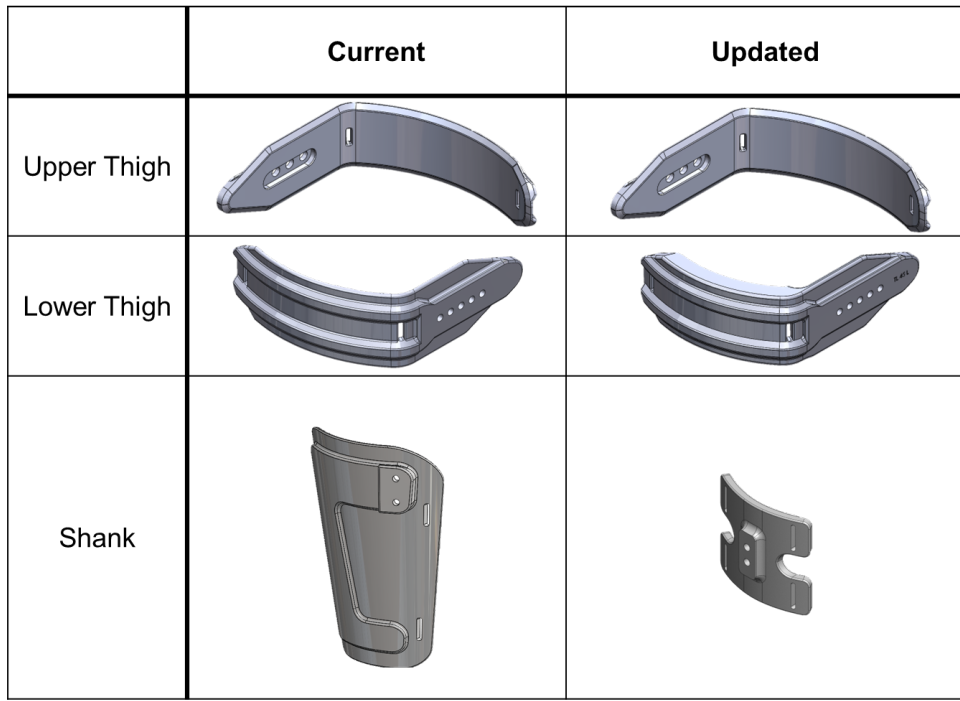


Figure 3.6: Comparison of the current wearable braces with the updated braces.

Table 3.3: Knee Exoskeleton Mass Comparison

Name	Current Version	New Version
	Mass (grams)	Mass (grams)
Upper thigh brace	146.98	145.52
Lower thigh brace	175.53	174.97
Thigh Bar	201.48	116.92
Actuator	780.00	600.00
Shank brace	184.90	116.15
Shank Assembly	82.57	134.95
Total	1571.46	1288.51

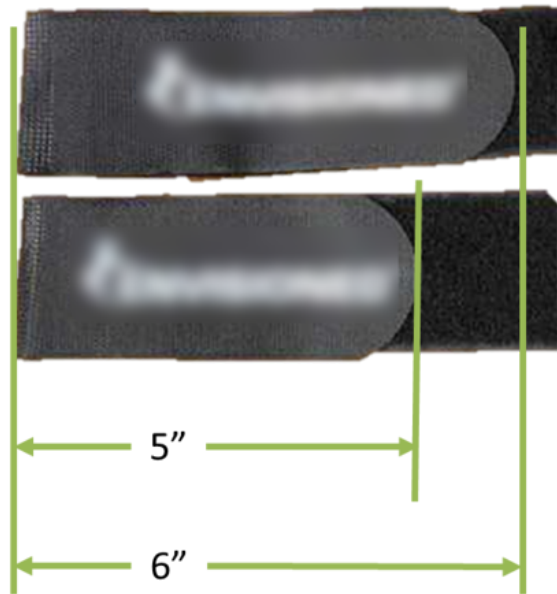


Figure 3.7: Shorten the hook pad for the Velcro straps to increase the range of fit.

To prevent the exoskeleton from slipping down the wearer's leg, a custom elastic band is used to support the exoskeleton from the waist band. The elastic band can be seen in Figure 3.8. The elastic band is made of bungee cord with metal snap clips. The cord is shaped and held in place to hold two large snap clips. One of the clips can be used to hook on the end of the exoskeleton while the entire band can loop over the waist band to allow the other snap clip to hook on the original snap clip. The bungee cord is able to provide a tension force that pulls the exoskeleton up to prevent the exoskeleton from sliding down. The extra circular snap clips are optional as their purpose is to adjust the overall length of the elastic band so that it is not too short that it is painful for the wearer or too long that it is not providing any tension. The overall weight of the elastic band itself averages at 35 g, but can increase by 2 to 5 g as more circular clips are added.



Figure 3.8: New elastic band design using bungee cord for tension and clip rings to adjust length.

### 3.3.3 Final Mechanical Design

The final knee exoskeleton is composed of one actuator per leg, support frames for the thigh and shank, and a waist-mount system, where the CAD model is described in Figure 3.9. The actuator transfers torque through the support frames to the user's knee joint. The support frames each fasten to the corresponding limb segment through a cuff with adjustable Velcro straps. An adjustable pre-tensioned elastic strap connects the support frames to a sturdy belt, which prevents the exoskeleton migrating down the legs and causing joint misalignment in the sagittal plane. H-shape hinge mechanism located on the shank support frame to provide better joint alignment and shank fit when the exoskeleton is moving. The 3D printed braces and soft, textile straps are modular and adjustable to ensure a good fit for a large range of physiques. These features together provide a comfortable experience for the wearer and reduce misalignment during torque assistance.

The knee joint actuator is uses the QDD actuator paradigm with a high torque density

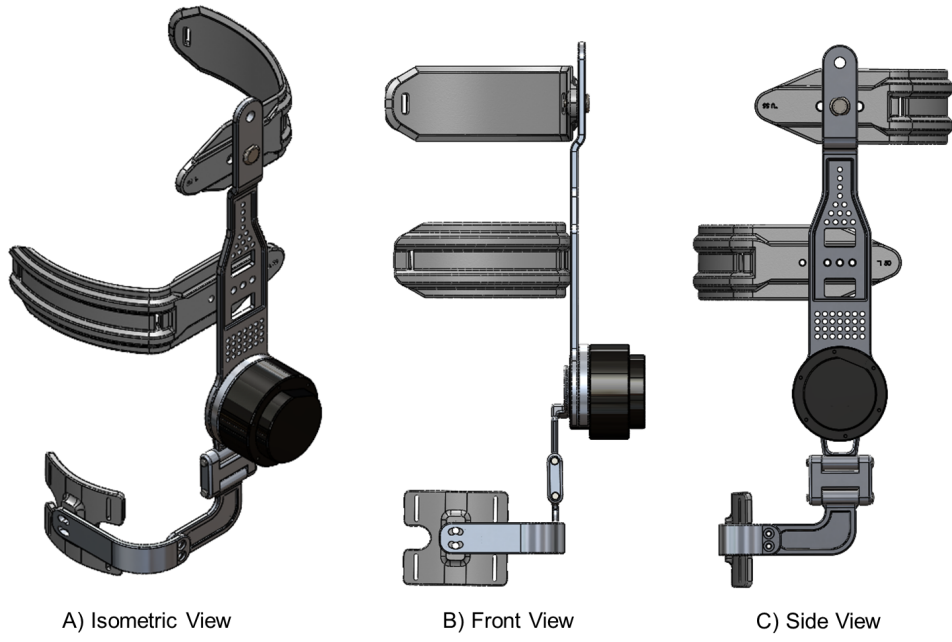


Figure 3.9: CAD model of the new version of knee exoskeleton.

actuator, torque sensor, and embedded system for low-level control. The custom torque sensor transfers torque loads from the actuator output stage to the shank support frame through bolted connections on each end. The exoskeleton is able to produce torque as much as 20 Nm. The sensor is rated for torques up to  $\pm 40$  Nm with a resolution of 0.1 Nm, staying well in the range of operations. The actuator provides a torque to the knee by transferring the force from the actuator through rigid an aluminum thigh bar and shank connector that is held in place by the custom straps.

The current knee exoskeleton's design and results has been done and published. Huang et al. (2022) The updated knee exoskeleton further improved on the current knee exoskeleton by reducing the overall weight, reducing the overall size, and providing ground clearance for kneeling tasks. A side by side comparison of the current exoskeleton with the updated exoskeleton can be seen in Figure 3.10

The updated mechanical parts were considered for their manufacturability. As one of

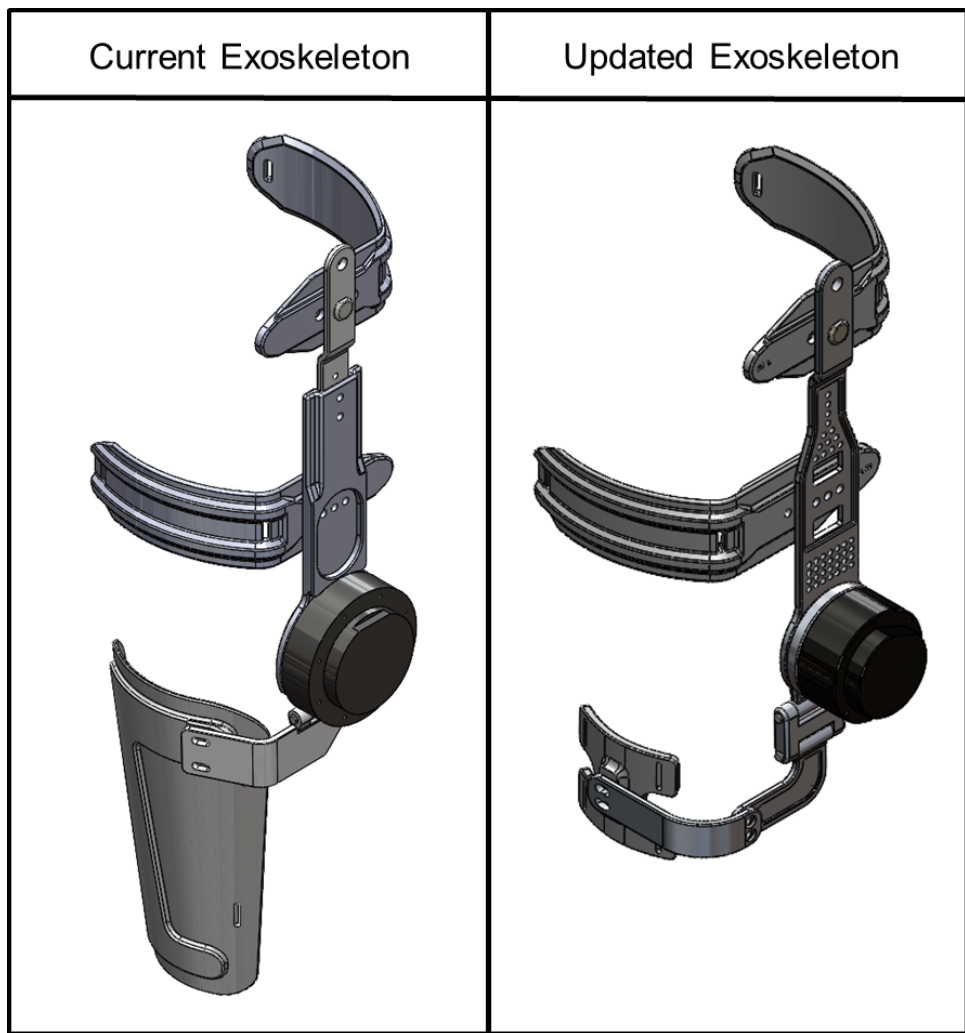


Figure 3.10: CAD model of the new version of knee exoskeleton.

the main support for the exoskeleton, the thigh bar has one of the most complex design mechanically. Ideally to further reduce the weight, more mass can be taken out of areas not encountering stress, such as in holed areas, however removing a large chunk of non circular shape of material is difficult for the shop, so a lattice form holes was used to make it easier to manufacture while still removing excess weight. The shank bar is also complex in shape due to the multiple bends to form around the shank. This is why the shank bar was separated into two separate parts since it is easier to manufacture a straight and a single bend part. The fully assembled exoskeleton can be seen in Figure 3.11.

### 3.4 Experimental Result

Since exoskeletons work in parallel with the wearer by providing an assistive force or torque at the targeted joint, the performance of the new version of knee exoskeleton was tested by how well the assistive torque matches, or tracks, the reference signal. The experiment was setup as a walking test with the exoskeleton with a healthy subject on the treadmill walking at a steady pace of 1.0 m/s. The experimental result can be seen in Figure 3.12.

The root mean square error (RMSE) between the reference torque and the actual measure torque was only 0.0754 Nm. The peak torque the exoskeleton can produced was roughly 10 Nm. Comparing the peak torque to the RMSE shows that there was only 0.754% difference which supports a high torque tracking accuracy. The reason the actual torque did not match the reference torque exactly is because regardless of how well the motor was designed, external mechanical parts will add additional dynamic complexities. No matter how much coding and tuning work is done there will always be a source of error and the tracking accuracy cannot reach as high as the tracking accuracy with just the actuator.

To check the backdrivability, or compliance, of the exoskeleton, the amount of torque it took to rotate the joint of the exoskeleton when the exoskeleton was commanded to provide

A) Final assembly



B) On legs



C) 2 Knee kneeling



D) 1 Knee kneeling



Figure 3.11: Final assembly of the new version of knee exoskeleton that is able to walk and kneel.

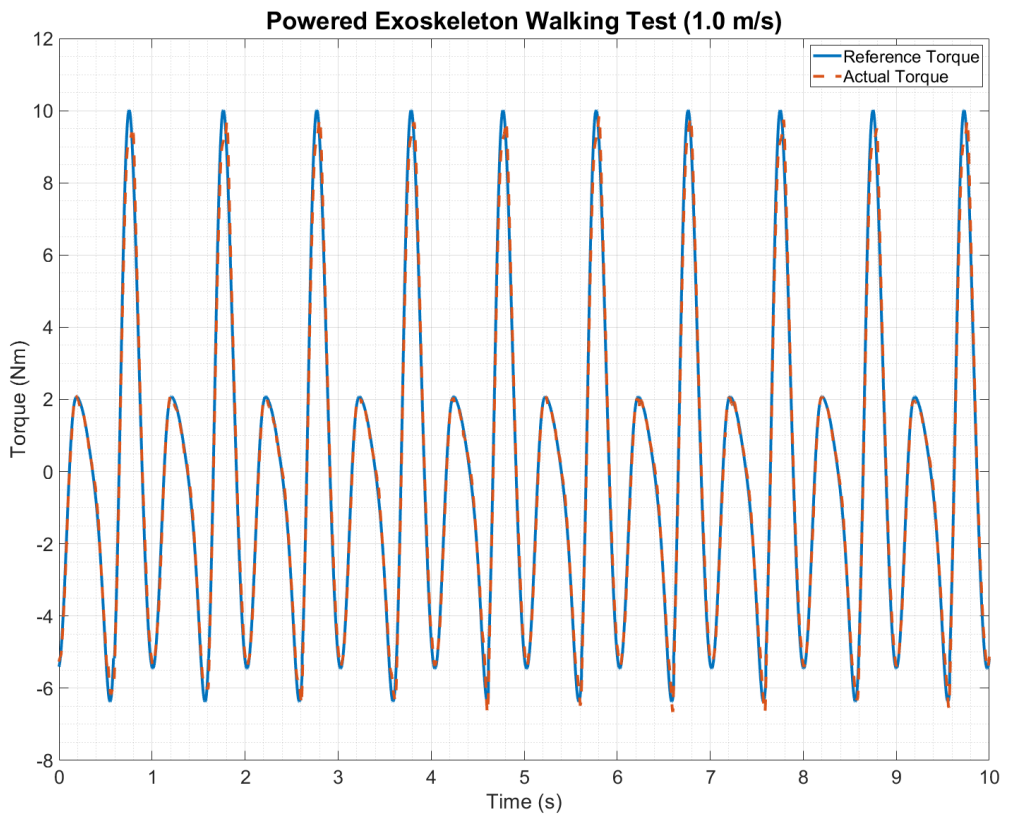


Figure 3.12: Torque tracking results with the newly designed knee exoskeleton with an RMSE of 0.0754 Nm.

zero torque was measured along with the position of the actuator. The exoskeleton was worn as usual with the torque sensor and encoder reading their respective measurements. The subject would bend their knee slowly at first while gradually increasing the speed. The results can be seen in Figure 3.13 where it showed that the amount of torque needed to move the unpowered actuator through approximately  $90^\circ$  was approximately 0.17 Nm. When compared to the 10 to 20 Nm applied by the exoskeleton during operation, 0.2 Nm is a relatively small value meaning the exoskeleton compliant enough where it would not change the natural kinematics of the wearer even during rapid movements.

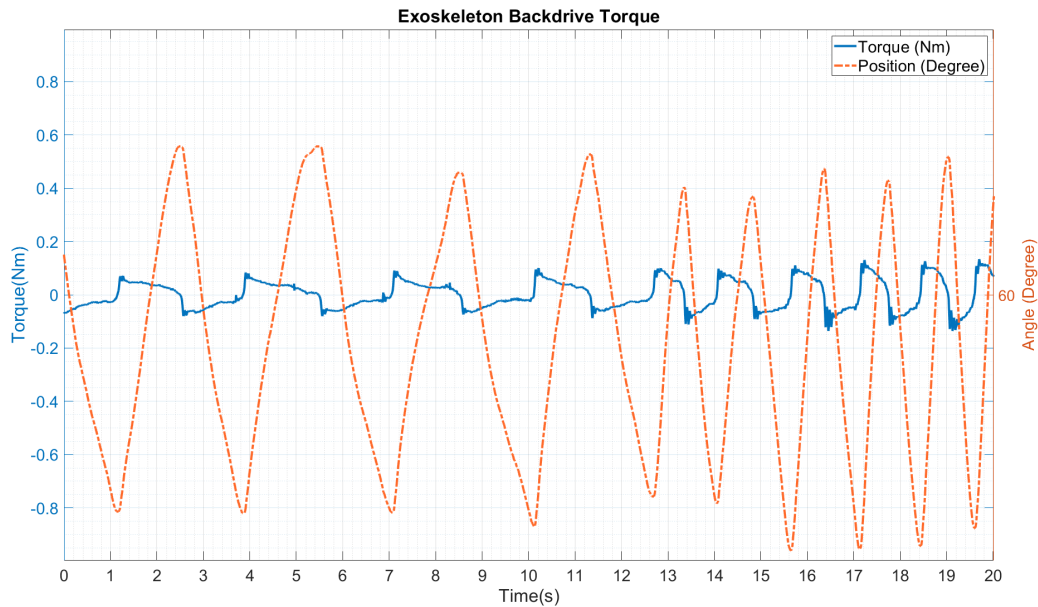


Figure 3.13: Measured the backdriving torque as the actuator was manually rotated where the max torque required was around 0.17 Nm.

## CHAPTER

### 4

# SOFT WEARABLE ROBOT - TETHERED ACTUATOR BASED EXOSKELETON

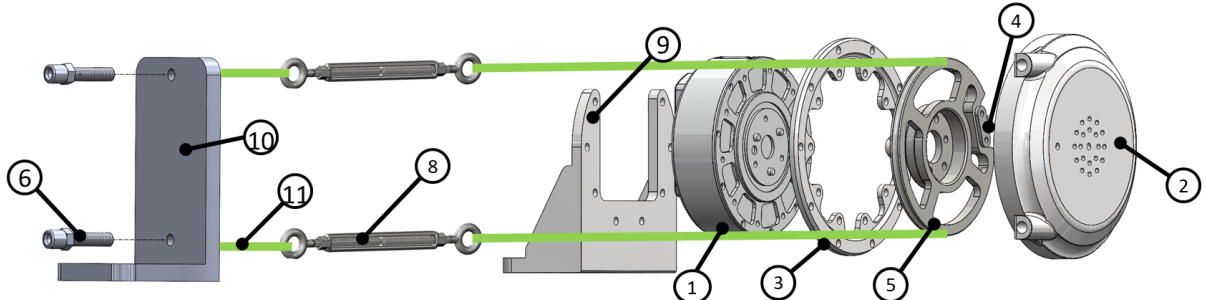
For some wearable robotic applications, sometimes the actuator cannot be collocated at the position due to certain design requirements. Most force transmission are done with heavy rigid parts such as sprocket and chain. Since mass is a crucial parameter in wearable robots, a lightweight, soft cable transmission system would be beneficial in the overall mechanical design. The actuation itself can act similar to contracting muscles which can be applied to many wearable robotic application where the user is lacking muscle strength. Some challenges with soft tethered transmission includes the mechanical backlash, cable

tension, and maximum force transmission. Soft cables are not as stable as more rigid metal cables. Soft cables are low in stiffness which can make their movements more chaotic to control when compared to a rigid metal cable with a higher stiffness. Since slack in the cable would not transmit any force, there needs to be a method to provide constant tension in the cable. Lastly, using a soft cable could also break much easier compared to a metal cable thus there is a force magnitude limit.

## 4.1 Mechanical Design

The actuator mount can be changed accordingly as its purpose is to hold the actuator to a stable platform, so the design can change depending on the application. The core components are the actuator, pulley loadcell, and the turnbuckle. The core idea is for the actuator to provide the torque to the cables where the turnbuckle is used to maintain tension from the actuator and the end unit with the pulley loadcell is able to measure the torque applied to the cable for torque control. Other parts in the tethered actuator assembly is the adaptor that connects the cover to the actuator, and cable housing screws that is used to connect bowden conduits to maintain a constant distance from the actuator to the end unit. The CAD model and assembly can be seen in Figure 4.1.

The goal of the tethered actuator is to use a soft cable as opposed to a rigid tether to reduce the mass and size of wearable robots. Rigid tethered transmission commonly uses a sprocket and chain design which can transfer high forces easily, but with soft tethered actuator, a pulley and fabric cable is used to greatly reduce the weight of the system but also reduces the amount of force that can be transmitted before breaking. Another challenge of soft tethered actuator is that most soft cables used stretches when in tension. This can cause slip and backlash from the actuator when it is reversing direction and the cable is no longer in tension. To overcome this problem, a soft fabric cable that is a Dyneema braided



Part Number	Part	Description	Quantity
1	RMD-X8 Pro	GYEMS actuator	1
2	Actuator cover	Aluminum cover for the actuator	1
3	Actuator adapter	Aluminum plate to connect the cover to the actuator	1
4	Cable holder	Stopper and mount for the cable	1
5	Pulley loadcell	Integrated loadcell with pulley to measure torque output	1
6	Cable housing screw	Bowden conduit housing with M8 thread with 2mm through hole for cable	2
7	Soft plug	Plug for cable hole in actuator cover	2
8	Turnbuckle	Adjust tension in the cable	2
9	Actuator mount	L-shaped bracket to mount the actuator	1
10	Tension bracket	L-shaped bracket to maintain tension	1
11	Braided cable	1.8mm fabric cable	2
12	Optical Table	Platform the system is built on	1

Figure 4.1: Bill of Materials for cable tethered system

cable was selected as the soft cable. Dyneema braided cable is resistant to stretching while being able to withstand a large amount of force in the cable. Shah et al. (2022) An assembled actuator can be seen in Figure 4.2. The actuator itself makes up the core of the total mass of the soft tether actuator where the total mass is around 885 grams. The mass can be further reduced by changing the aluminum cover and adapter to plastic since their main purpose is to keep the cable lined up on the pulley.

## 4.2 Sensor and Calibration

Since the main purpose of the soft tethered actuator is to transmit force, the easiest way to control the actuator is to use torque control which requires a torque feedback to accurately track the reference signal. A pulley loadcell is used to measure the torque applied from the actuator, but the loadcell itself needs to be calibrated to measure the correct torque.

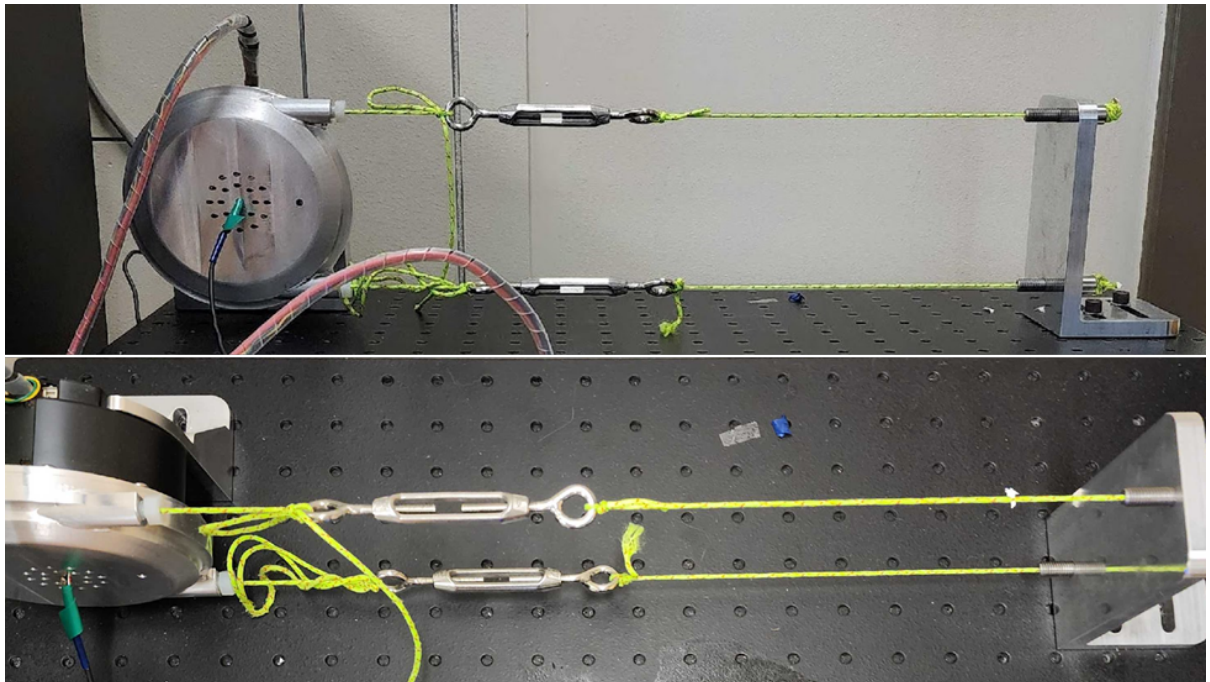


Figure 4.2: Final assembly for the soft tethered actuator.

The loadcell measures the torque that is acting on it and sends the measurement as a low voltage analog signal. The signal would increase in magnitude with the increase in the torque applied, but this does not mean the voltage signal reading equals the torque applied. By changing the magnitude of the voltage signal is read to equal the expected torque, the loadcell will be able to accurately measure the torque applied on the loadcell.

There are two methods of calibrating the loadcell. First method is a manual calibration with a known torque source, and the second method is using the actuator's torque constant. An example of sensor calibration can be seen in Figure 4.3. The loadcell is held in place on an optical table with a rigid beam of a known length with a known mass hanging at the end. Using the moment formula, equation 4.1, where the mass causes a force on the beam due to gravity, the total torque experienced by the loadcell can be calculated. Using the example shown in Figure 4.3, the loadcell should be experiencing roughly 7.35 Nm torque.

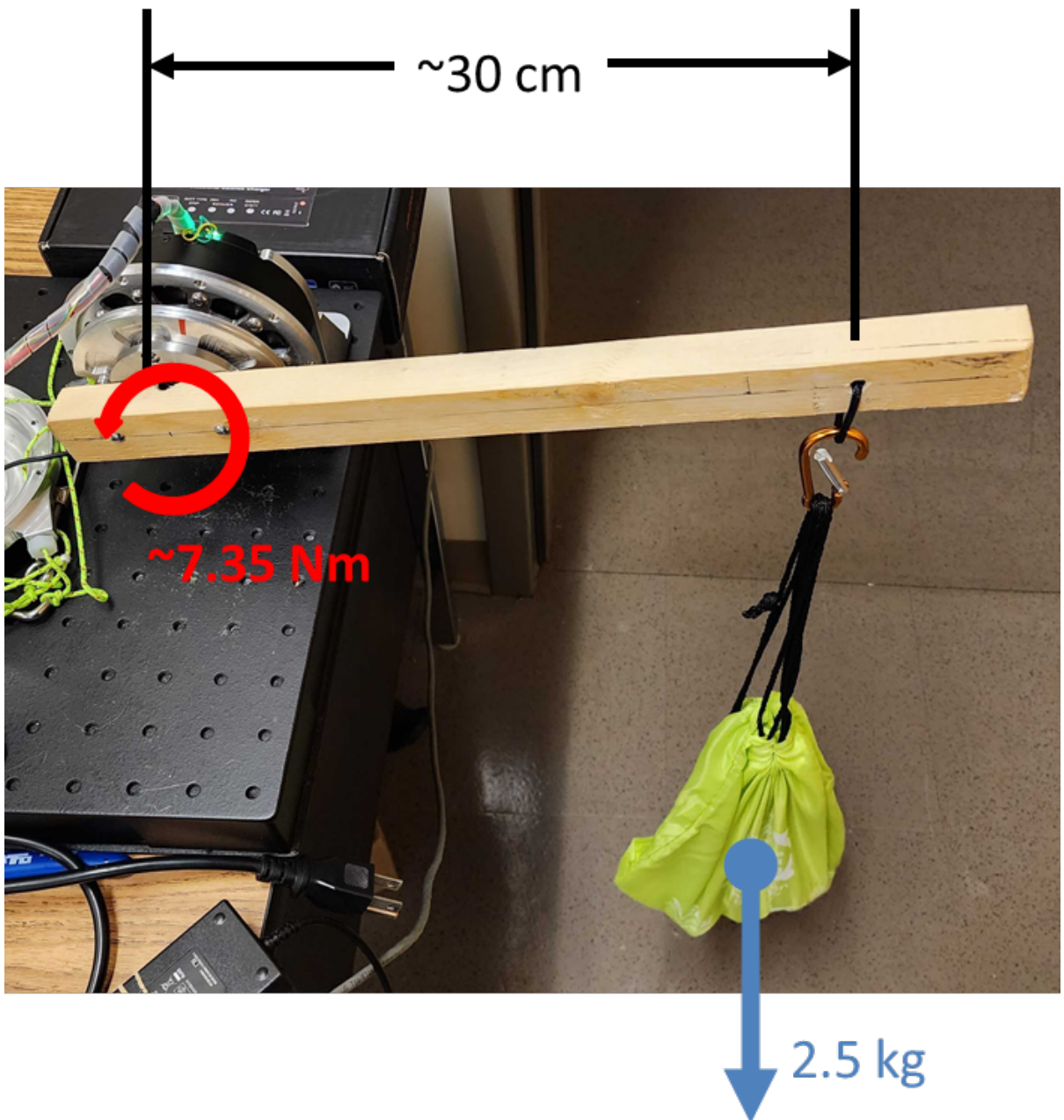


Figure 4.3: Loadcell calibration using a known torque source.

$$\begin{aligned}\tau &= mg r \\ \tau &= (2.5\text{kg})(9.81\text{m/s}^2)(0.3\text{m}) = 7.3575\text{Nm}\end{aligned}\tag{4.1}$$

For equation 4.1,  $\tau$  is the torque applied by the hanging mass,  $m$  is the mass,  $g$  is the gravitational acceleration, and  $r$  is the distance the mass is from the center of the loadcell.

The second method of calibrating the loadcell is using the known torque constant provided. The loadcell must be held in place while the actuator applies a constant torque from a constant current. The applied torque can be calculated with equation 4.2.

$$\tau = K_\tau I n\tag{4.2}$$

$\tau$  is still the torque but the source is from the actuator using a constant current.  $I$  is the current drawn by the actuator,  $n$  is the gear ratio of the actuator, and  $K_\tau$  is the torque constant of the motor. The gear ratio needs to be considered because the torque constant applies to how much torque the motor provides during direct drive meaning there are no gear box. For the QDD actuator, the gear box is built into the entire actuator system, so the gear ratio needs to be considered when measuring the actual torque produced from a constant current.

### 4.3 Experiments

To ensure the tracking accuracy of the actuator, a torque tracking experiment was run on the soft tethered actuator. Due to the mechanical complexity of the additional soft

cable and pulley loadcell, the PID tuning of the system can be difficult with just the base micro-controller architecture, so a real-time machine (Simulink real-time target machine, Speedgoat) was used as the high level computer to better tune and control the tethered actuator. The experiment setup can be seen in Figure 4.4.

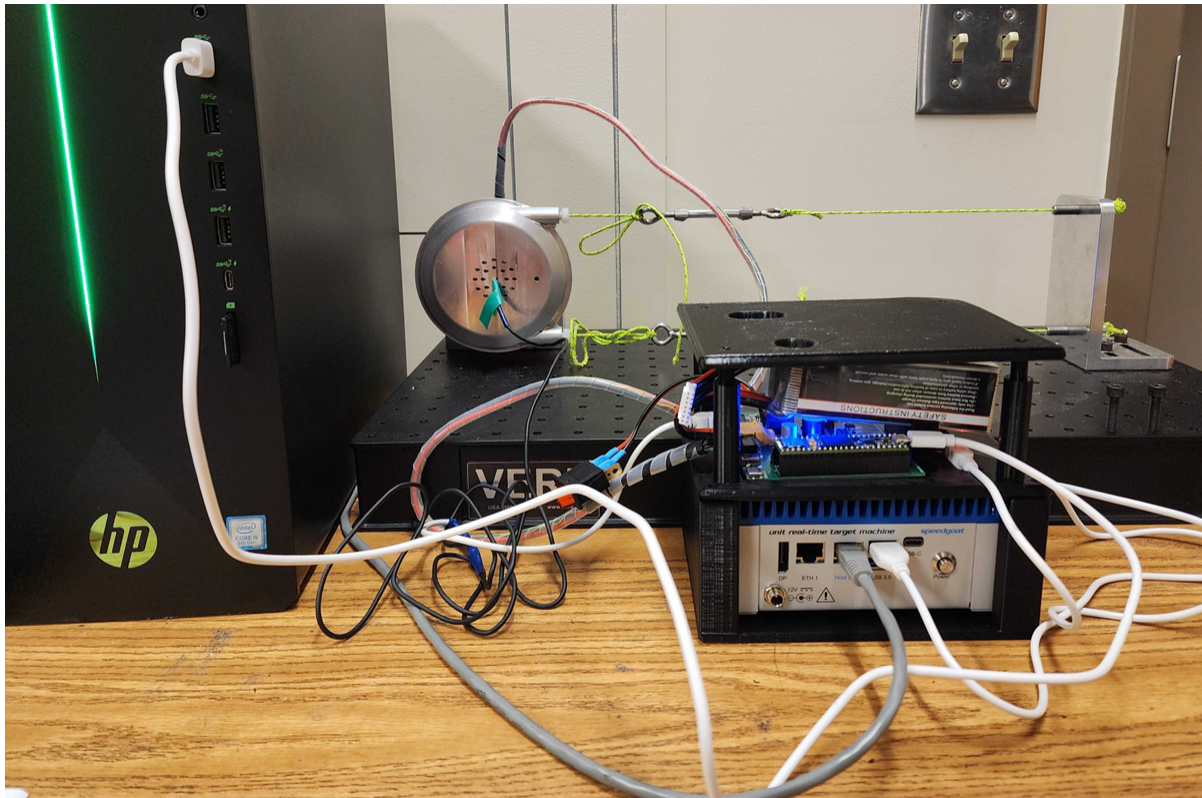


Figure 4.4: Experimental setup for the soft tethered cable actuator.

The bench-top test is done by sending two separate torque wave function with an amplitude of 10 Nm and 15 Nm at 1 hertz. A wave function was used to simulate the periodicity of human motion. The results of the experiments for 10 Nm and 15 Nm can be seen in Figure 4.5 and Figure 4.6 respectively. The RMSE between the reference torque and the actual torque is approximately 0.008 Nm for the 10 Nm torque tracking and 0.011

Nm for 15 Nm torque tracking. When comparing the RMSE to the peak torque, there is a 0.08% difference with 10 Nm test and a 0.073% difference with the 15 Nm test. These results support the high accuracy of the soft tethered actuator since the percent difference is less than 0.1%. The tracking for the tethered torque tracking did have a small increase of error, but this was expected as the cable and pulley increased in mechanical complexity. The error difference, however, is small, and the tethered actuator was still able to produce a highly accurate torque tracking results.

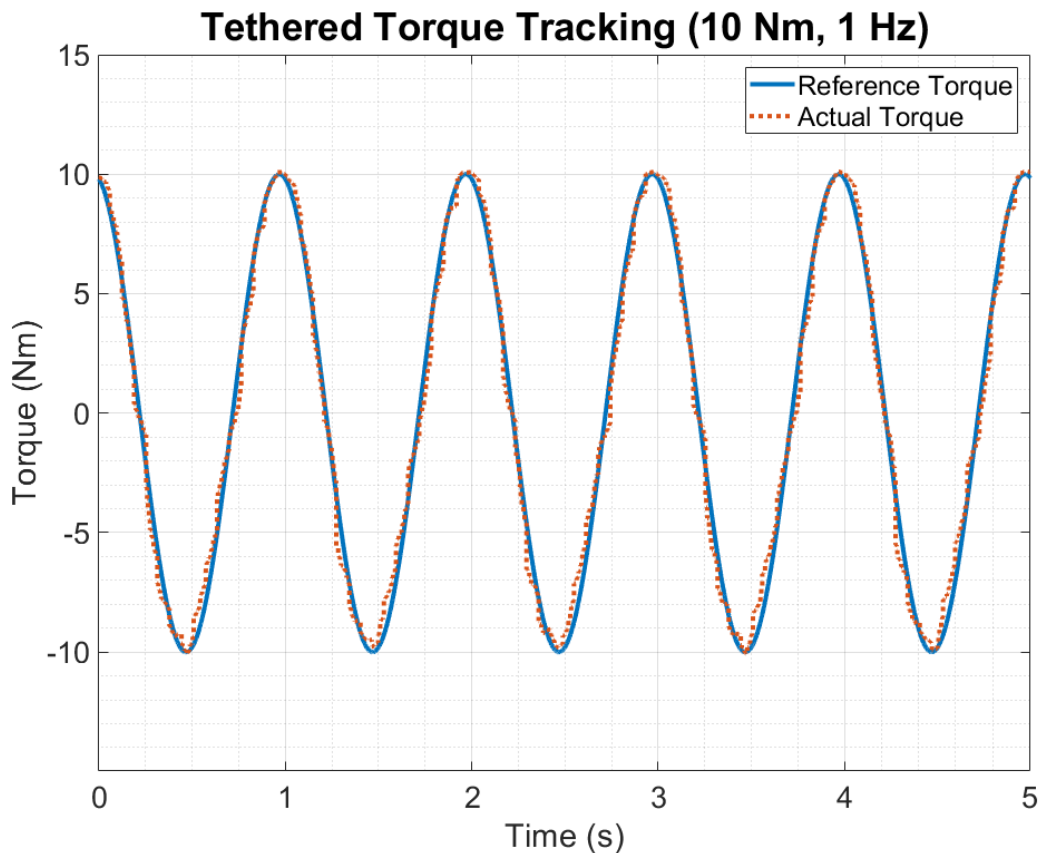


Figure 4.5: Torque tracking result for a 10 Nm 1 Hz wave reference signal with a RMSE of 0.008 Nm

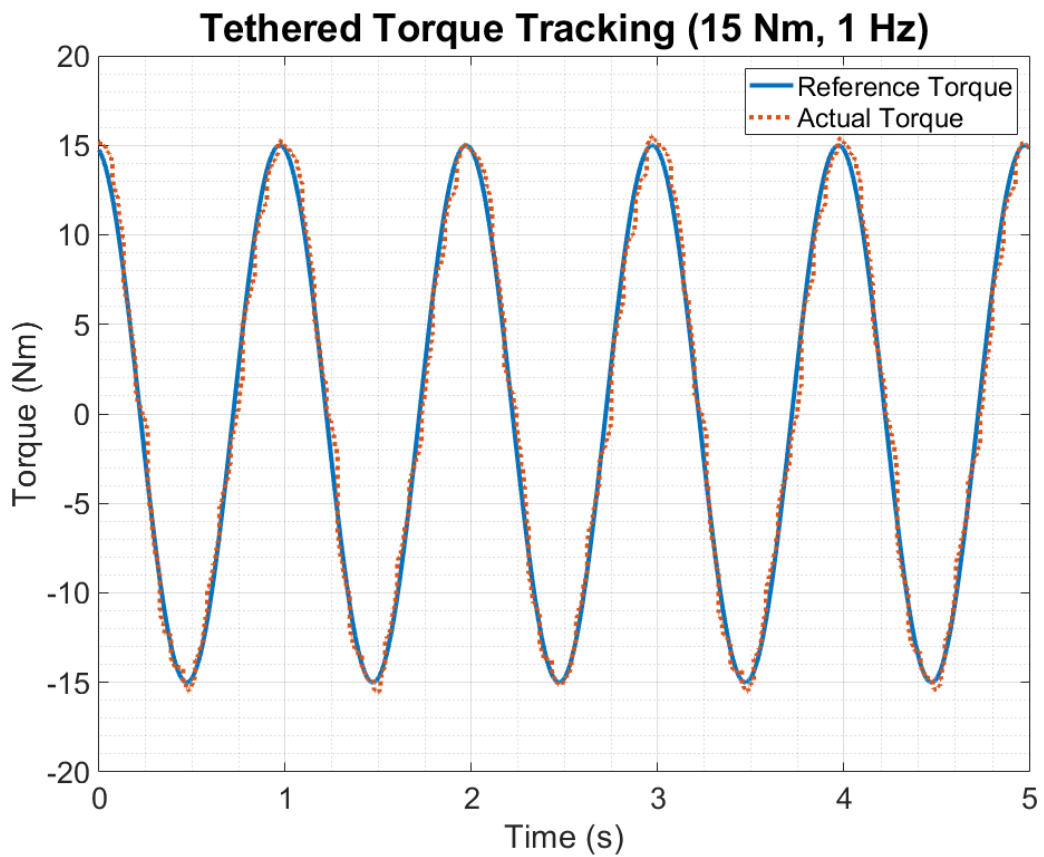


Figure 4.6: Torque tracking result for a 15 Nm 1 Hz wave reference signal with a RMSE of 0.011 Nm

## 4.4 Application

The benefit of using the soft tethered actuator is that the actuator itself is not limited to the area of actuator and that the assistive force acts similar to contracting muscles. For a joint with a large degree of freedom, such as the wrist, a singular actuator located at the joint cannot provide the proper assistance and would hinder the wearer's natural movements, so using a soft tethered actuator is able to transfer assistive forces to the hands through the tension in the cables that acts similar to an additional muscle. Without the additional mass of an actuator at the wrist also allows for flexible and natural movement from the wearer since only the cable anchors exist near the wrist. The lab's wrist exoskeleton can be seen in Figure 4.7.



Figure 4.7: Wrist exoskeleton using a soft tethered actuator that can be used to help open containers for users with arthritis.

The high accuracy of the soft tethered actuator can provide a more flexible design option for wearable robots since the physical actuator itself is not limited to the targeted area on the body as seen in the wrist exoskeleton where the physical actuators is mounted on the back. This actuation paradigm is not limited to upper limb exoskeletons since lower limb exoskeletons may also need a centralize actuator position to improve the user's comfort and decrease the mass penalty. Tethered system is also commonly used in portable exosuits, and the lightweight nature of the soft tethered actuator can improve the mechanical design of the exosuit. Bae et al. (2018)

## CHAPTER

# 5

## OTHER APPLICATIONS

Aside from the knee exoskeleton and soft tethered actuator, other types of wearable robots have also been developed by the BIRO Lab, such as the hip exoskeleton, shoulder exoskeleton, and trans-femoral prosthesis. Though the general structure for each type of wearable robot is similar, such as actuator with a rigid frame, the design details varies greatly to suit each individual wearable robot. The first design consideration always start with the user because of humans are part of wearable robotic system, and future design consideration should always ensure the user's safety, natural movements, and benefits. Many emergency and safety features should be included in the design, but they should be the guaranteed fail safes which means the functionality of the wearable robot should be safe for humans regardless. Aside from the safety concerns, the wearable robot does impose

an additional mass and inertia on the wearable which can affect their natural kinematics. Witte and Collins (2020) This means the mechanical design of wearable robots should be as light as possible while having high compliance. A lighter wearable robot would have a smaller metabolic effect on the wearer while having high compliance allows more freedom of movement for the wearer. The control strategies of wearable robots are also important. Because of the variation in the type of movement and how the wearer move, quick and adaptable response to the wearer are needed to not only ensure the safety of the wearer but also to provide the proper assistance to the wearer. QDD actuators are chosen to meet these design requirements of high torque, high compliance, lightweight, and high bandwidth which has been tested in previous works. Yu et al. (2020), Nesler et al. (2022) This is also a challenge in moving the exoskeleton out of clinical setting and into community settings because the environment is also another source of input to the robotic system that has more variability.

## 5.1 Hip Exoskeleton

For an exoskeleton to be assistive to the user, the assistive torque must be applied properly since applying a torque at an improper time can severely hurt or trip the wearer. The control system for the exoskeleton is designed around this goal. An exoskeleton's control system framework is broken down into three levels (high, mid, and low levels). High level control involves with recognizing the user's intent. For a LLE, its high level control deals with the user's gait estimation. The reference from the high level control is passed down to the mid level where the proper movement or torque is calculated. After calculating the proper command in the mid level, the reference command is passed down to the lower level where the command is executed accurately. The low level control usually involves the actuation mechanism where control methods, such as PID control, is used to ensure high accuracy

between the input and output. Azocar et al. (2020a)

The hip joint is the most proximal joint of the lower limb joint which mean the assistance here can affect the distal joints further down the limbs due to the assistive torque effects on the muscles at the hip. During a normal gait cycle, the hip joint requires more biological moment than the knee joint to create movement since it is moving the entire limb. The hip exoskeleton uses a similar actuation paradigm to the knee exoskeleton. There is one actuator per side that is supported by the electronic box frame on the waist-mount system. Torque is transferred to the hip joint by the rigged bar that is connected to the thigh by Velcro padded belt from the actuator. Because the actuators and the electronics are at the hips, there is no need to use elastic bands to support the main structure. The waist band can hold the exoskeleton due to the shape at the waist since the diameter increases towards the hips, so the body can support the exoskeleton without it sliding down. The structure at the thighs transfers the torque provided by the actuator with a rigid 3D printed brace that is held in place by a Velcro padded belt on each thigh.

The QDD actuators are attached on each side of the wearer's hip with a passive joint to adapt to varying abduction movements in the hip. A custom designed waist band, where the electronics box is also attached, supports the entire exoskeleton. The waist band is made of rigid aluminum parts and soft fabric padding. The rigid parts are able to transfer the torque produced by the actuator to the wearer while the soft padding prevents the rigid aluminum part from hurting the wearer. From the actuator, another custom aluminum bar is connected to the center on the thigh's surface that is held in place using a strip of padding with Velcro. The CAD model can be seen in Figure 5.1

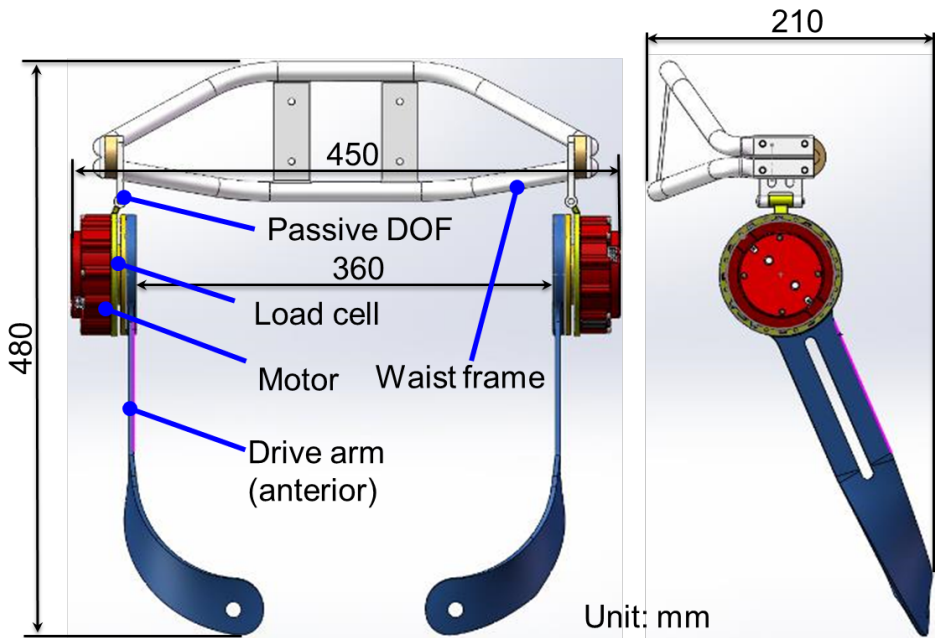


Figure 5.1: CAD model of the hip exoskeleton

## 5.2 Shoulder Exoskeleton

The purpose of upper limb exoskeletons differs greatly from lower limb exoskeletons not only in the joint locations. To provide resistance to fatigue due to repetitive activities, such as lifting, pushing, and pulling, an upper limb exoskeleton, such as the shoulder exoskeleton, can provide an assistive force to make repetitive tasks easier for the wearer. Shang et al. (2017) Shoulder exoskeleton can also be used for rehabilitation purposes for patients that are paralyzed or have difficulties moving their arms due to injury or stroke and would be able to help restore some motor functions. Sharma and Ordonez (2016)

The shoulders joint behavior affects the whole arm which means it not only direct the majority of the upper limbs' movement, it also has an effect on the fine motor movements in the hands. Due to the multiple degrees of freedom in the shoulder, a single actuator at the shoulder joint is insufficient in providing the proper assistance needed for natural

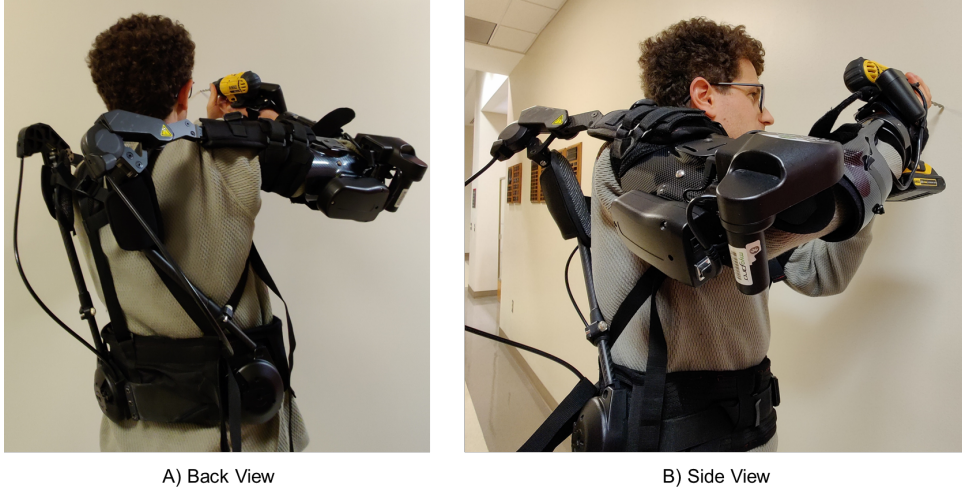


Figure 5.2: Back and side views of the shoulder exoskeleton that also uses a soft tethered actuator.

movement. Thus the actuation method uses a cable tethered actuator that allow for free movement at the shoulders while still providing assistance to the shoulder. The QDD actuator is mounted on the waist belt of the exoskeleton with two cables feeding up the back through aluminum links and over the shoulder before the upper cable is mounted to the top of the upper arm and the lower cable is mounted to the bottom of the upper arm. As the actuator rotates, the cables pulls on the upper arm acting similar to a contracting muscle that causes shoulder flexion or extension depending on if the upper or lower cable is pulling. The lab's shoulder exoskeleton can be seen in Figure 5.2

### 5.3 Trans-femoral Prostheses

To assist trans-femoral amputees with their mobility problems, patients would use passive, semi-passive, or powered prostheses as the solution to their mobility problem. Passive prostheses are often used due to their low cost and lightweight simplicity but cannot support the user in more robust activities; however, due to their rigid design, they only

support their walking and not enhancing them. Zhu et al. (2022) Powered prostheses are available to fill this gap in need by providing the mobility assistance in a more robust and natural way. Azocar et al. (2018), Azocar et al. (2020b) Similar to exoskeletons, powered prosthesis is also a type of wearable robot, but instead of working in parallel with the wearer like an exoskeleton, prostheses work in series. This means that instead of matching the wearer's locomotion, prostheses attempts replace the missing motion which is guided by a more proximal joint. Our lab's powered prosthesis can be also controlled using the same electronics architecture. The prosthesis itself is also relatively lightweight with its total mass being around 3.3 kg. The prosthesis' actuation uses a similar high density torque QDD actuator (T-Motor AK10-9) as the exoskeletons that accounts for the majority of the mass of the prosthesis. The wearer can strap on the prosthesis at the end of the thigh using velcro straps with a realistic footplate the end of the prosthesis. The designed prosthesis can be seen in Figure 5.3. The L-shaped brace was mainly used for healthy individual testing, but for amputees a similar brace would be used without the additional support at the shank that was needed for healthy individual testing. The actuator is also compliant and backdrivable making it more comfortable for the wearer. By not using a high gear ratio gearbox, it eliminates the need for constant maintenance, high decibel noises, and efficiency penalties due to friction from the gear teeth.



Figure 5.3: Front and side views of the trans-femoral prosthesis.

## CHAPTER

# 6

## CONCLUSION AND FUTURE WORK

This thesis introduces a flexible electronic architecture design that can be used to control and operate with different types of wearable robots while also being compatible with different types of high-level computers, such as JPU or Simulink Real-Time Machine, while still being able to be powered by a battery and small enough to be portable without hindering the wearer's natural movements. The core of the electronics architecture is the custom PCB. All the sensor ports and connections are already built in on the PCB but does not require the connection of unnecessary sensors or peripherals with they are unused without the need to change the hardware or software. The same electronics and sensor can be used to control multiple types of exoskeleton at different joints regardless if it is a prosthesis or exoskeleton, and whether the exoskeletons are lower limb or upper limb. It also intro-

duces the mechanical designs of BIRO lab's wearable robots that includes lower and upper limb exoskeletons as well as lower limb prosthesis. Each wearable robot is designed to be lightweight and backdrivable by utilizing the unique characteristics of a QDD actuator. Updates to the knee exoskeleton was also done to provide ground clearance when kneeling and better comfort for the shank brace.

## REFERENCES

- Azocar, A., Mooney, L., Duval, J.-F., Simon, A., Hargrove, L., and Rouse, E. (2020a). Design and clinical implementation of an open-source bionic leg. *Nature Biomedical Engineering*, 4:1–13.
- Azocar, A. F., Mooney, L. M., Duval, J.-F., Simon, A. M., Hargrove, L. J., and Rouse, E. J. (2020b). Design and clinical implementation of an open-source bionic leg. *Nature Biomedical Engineering*, 4(10):941–953.
- Azocar, A. F., Mooney, L. M., Hargrove, L. J., and Rouse, E. J. (2018). Design and characterization of an open-source robotic leg prosthesis. In *2018 7th IEEE International Conference on Biomedical Robotics and Biomechatronics (Biorob)*, pages 111–118.
- Bae, J., Siviy, C., Rouleau, M., Menard, N., O'Donnell, K., Geliana, I., Athanassiu, M., Ryan, D., Bibeau, C., Sloot, L., Kudzia, P., Ellis, T., Awad, L., and Walsh, C. J. (2018). A lightweight and efficient portable soft exosuit for paretic ankle assistance in walking after stroke. In *2018 IEEE International Conference on Robotics and Automation (ICRA)*, pages 2820–2827.
- Bulea, T. C., Molazadeh, V., Thurston, M., and Damiano, D. L. (2022). Interleaved assistance and resistance for exoskeleton mediated gait training: Validation, feasibility and effects. pages 1–8.
- Cao, W., Ma, Y., Chen, C., Zhang, J., and Wu, X. (2022). Hardware circuits design and performance evaluation of a soft lower limb exoskeleton. *IEEE Transactions on Biomedical Circuits and Systems*, 16(3):384–394.
- Chen, J., Hochstein, J., Kim, C., Damiano, D., and Bulea, T. (2018). Design advancements toward a wearable pediatric robotic knee exoskeleton for overground gait rehabilitation. In *2018 7th IEEE International Conference on Biomedical Robotics and Biomechatronics (Biorob)*, pages 37–42.
- Chen, S., Stevenson, D. T., Yu, S., Mioskowska, M., Yi, J., Su, H., and Trkov, M. (2021). Wearable knee assistive devices for kneeling tasks in construction. *IEEE/ASME Transactions on Mechatronics*, 26(4):1989–1996.
- Dunkelberger, N., Berning, J., Dix, K. J., Ramirez, S. A., and O'Malley, M. K. (2022). Design, characterization, and dynamic simulation of the mahi open exoskeleton upper limb robot. *IEEE/ASME Transactions on Mechatronics*, 27(4):1829–1836.
- Duval, J.-F. and Herr, H. M. (2016). Flexsea: Flexible, scalable electronics architecture for wearable robotic applications. In *2016 6th IEEE International Conference on Biomedical Robotics and Biomechatronics (BioRob)*, pages 1236–1241.

- Huang, T.-H., Zhang, S., Yu, S., MacLean, M. K., Zhu, J., Di Lallo, A., Jiao, C., Bulea, T. C., Zheng, M., and Su, H. (2022). Modeling and stiffness-based continuous torque control of lightweight quasi-direct-drive knee exoskeletons for versatile walking assistance. *IEEE Transactions on Robotics*, 38(3):1442–1459.
- Jayaraman, A., O'Brien, M., Madhavan, S., Mummidisetti, C., Roth, H., Hohl, K., Tapp, A., Brennan, K., Kocherginsky, M., Williams, K., Takahashi, H., and Rymer, W. (2018). Stride management assist exoskeleton vs functional gait training in stroke: A randomized trial. *Neurology*, 92:10.1212/WNL.0000000000006782.
- Kutzner, I., Heinlein, B., Graichen, F., Bender, A., Rohlmann, A., Halder, A., Beier, A., and Bergmann, G. (2010). Loading of the knee joint during activities of daily living measured in vivo in five subjects. *Journal of Biomechanics*, 43(11):2164–2173.
- Lerner, Z. F., Damiano, D. L., and Bulea, T. C. (2017a). A lower-extremity exoskeleton improves knee extension in children with crouch gait from cerebral palsy. *Science translational medicine*, 9(404).
- Lerner, Z. F., Damiano, D. L., Park, H.-S., Gravunder, A. J., and Bulea, T. C. (2017b). A robotic exoskeleton for treatment of crouch gait in children with cerebral palsy: Design and initial application. *IEEE Transactions on Neural Systems and Rehabilitation Engineering*, 25(6):650–659.
- Lv, G., Zhu, H., and Gregg, R. D. (2018). On the design and control of highly backdrivable lower-limb exoskeletons: A discussion of past and ongoing work. *IEEE Control Systems Magazine*, 38(6):88–113.
- Nesler, C., Thomas, G., Divekar, N., Rouse, E. J., and Gregg, R. D. (2022). Enhancing voluntary motion with modular, backdrivable, powered hip and knee orthoses. *IEEE Robotics and Automation Letters*, 7(3):6155–6162.
- Nesler, C., Thomas, G. C., Divekar, N., Rouse, E. J., and Gregg, R. D. (2021). Enhancing voluntary motion with modular, backdrivable, powered hip and knee orthoses. *CoRR*, abs/2110.01562.
- Plaza, A., Hernandez, M., Puyuelo, G., Garces, E., and Garcia, E. (2023). Lower-limb medical and rehabilitation exoskeletons: A review of the current designs. *IEEE Reviews in Biomedical Engineering*, 16:278–291.
- Shah, A. A., Shahid, M., Hardy, J. G., Siddiqui, N. A., Kennedy, A. R., Gul, I. H., Rehman, S. U., and Nawab, Y. (2022). Effects of braid angle and material modulus on the negative poisson's ratio of braided auxetic yarns. *Crystals*, 12(6):781.
- Shang, K., Xu, X., and Su, H. (2017). Design and evaluation of an upper extremity wearable robot with payload balancing for human augmentation. In *2017 International Symposium on Wearable Robotics and Rehabilitation (WeRob)*, pages 1–1.

- Sharma, M. K. and Ordonez, R. (2016). Design and fabrication of an intention based upper-limb exo-skeleton. In *2016 IEEE International Symposium on Intelligent Control (ISIC)*, pages 1–6.
- Tucker, L. A., Chen, J., Hammel, L., Damiano, D. L., and Bulea, T. C. (2020). An open source graphical user interface for wireless communication and operation of wearable robotic technology. *Journal of Rehabilitation and Assistive Technologies Engineering*, 7:205566832096405.
- Wensing, P. M., Wang, A., Seok, S., Otten, D., Lang, J., and Kim, S. (2017). Proprioceptive actuator design in the mit cheetah: Impact mitigation and high-bandwidth physical interaction for dynamic legged robots. *IEEE Transactions on Robotics*, 33(3):509–522.
- Witte, K. A. and Collins, S. H. (2020). Chapter 13 - design of lower-limb exoskeletons and emulator systems. In Rosen, J. and Ferguson, P. W., editors, *Wearable Robotics*, pages 251–274. Academic Press.
- Yu, S., Huang, T.-H., Di Lallo, A., Zhang, S., Wang, T., Fu, Q., and Su, H. (2022). Bio-inspired design of a self-aligning, lightweight, and highly-compliant cable-driven knee exoskeleton. *Frontiers in Human Neuroscience*, 16.
- Yu, S., Huang, T.-H., Wang, D., Lynn, B., Sayd, D., Silivanov, V., Park, Y. S., Tian, Y., and Su, H. (2019). Design and control of a high-torque and highly backdrivable hybrid soft exoskeleton for knee injury prevention during squatting. *IEEE Robotics and Automation Letters*, 4(4):4579–4586.
- Yu, S., Huang, T.-H., Yang, X., Jiao, C., Yang, J., Chen, Y., Yi, J., and Su, H. (2020). Quasi-direct drive actuation for a lightweight hip exoskeleton with high backdrivability and high bandwidth. *IEEE/ASME Transactions on Mechatronics*, 25(4):1794–1802.
- Yu, S., Yang, J., Huang, T.-H., Zhu, J., Visco, C. J., Hameed, F., Stein, J., Zhou, X., and Su, H. (2023). Artificial neural network-based activities classification, gait phase estimation, and prediction. *Annals of Biomedical Engineering*, pages 1–14.
- Zhang, J., Fiers, P., Witte, K. A., Jackson, R. W., Poggensee, K. L., Atkeson, C. G., and Collins, S. H. (2017). Human-in-the-loop optimization of exoskeleton assistance during walking. *Science*, 356(6344):1280–1284.
- Zhu, J., Jiao, C., Dominguez, I., Yu, S., and Su, H. (2022). Design and backdrivability modeling of a portable high torque robotic knee prosthesis with intrinsic compliance for agile activities. *IEEE/ASME Transactions on Mechatronics*, 27(4):1837–1845.

## **APPENDICES**

## APPENDIX

### A

### ACRONYMS

A summary of all acronyms is documented in Table A.1.

Table A.1: A summary of acronyms used in alphabetical order.

Acronym	Abbreviation
Analog to Digital Convertor	ADC
Controller Area Network	CAN
Cerebral Palsy	CP
Finite Element Analysis	FEA
Graphical User Interface	GUI
Ground Force Reaction	GRF

High-Definition Multimedia Interface	HDMI
Inertial Measurement Unit	IMU
Jetson Processing Unit	JPU
Lower Limb Exoskeleton	LLE
Printed Circuit Board	PCB
Proportional Integral Derivative	PID
Quasi-Direct Drive	QDD
Root Mean Square Error	RMSE
Serial Peripheral Interface	SPI
Universal Asynchronous Receiver/Transmitter	UART

## APPENDIX

### B

### UNITS

A summary of all units is documented in Table B.1.

Table B.1: A summary of units used in alphabetical order.

Units	Abbreviation
Ampere	A
Centimeter	cm
Gram	g
Hertz	Hz
Hour	hr
Kilogram	kg

Meter	m
Millimeter	mm
Newton	N
Pascal	Pa
Radian	rad
Second	s
Voltage	V